Alma Mater Studiorum - Università di Bologna

DOTTORATO DI RICERCA IN

SCIENZE BIOMEDICHE E NEUROMOTORIE

Ciclo 35

Settore Concorsuale: 06/D3 - MALATTIE DEL SANGUE, ONCOLOGIA E REUMATOLOGIA

Settore Scientifico Disciplinare: MED/06 - ONCOLOGIA MEDICA

A 3D BIOMIMETIC IN VITRO MODEL: A NOVEL STRATEGY TO INVESTIGATE GLIOMA BIOLOGY

Presentata da: Claudia Cocchi

Coordinatore Dottorato

Matilde Yung Follo

Supervisore

Laura Mercatali

Co-supervisore

Pietro Cortelli

Esame finale anno 2023

Abstract

Brain tumors account for 85% to 90% of all primary central nervous system (CNS) tumors. Gliomas are the most frequent primary malignant brain tumors in adults with an estimated incidence of 7.1/100,000 cases every year in the United States. The World Health Organization (WHO) 2021 classification mainly divided gliomas into isocitrate dehydrogenase (IDH) mutant and IDH wild-type tumors, from which derived various subgroup, based on an integration of the established immunohistochemical analysis with the molecular investigation to a better patients' stratification. Acquisition of stem-like features likely contributes to the malignant nature of high-grade gliomas and may be responsible for the initiation, growth, and recurrence of these tumors. In this regard, although the traditional two-dimensional (2D) cell culture system has been widely used in cancer research, it shows limitations in maintaining the stemness properties of cancer and in mimicking the *in vivo* microenvironment. These issues are partially responsible for the gap existing between preclinical and clinical results. In order to overcome these limitations, different three-dimensional (3D) culture systems have been developed to mimic better the tumor microenvironment. In particular, cancer cells cultured in 3D structures may represent a more reliable *in vitro* model due to increased cell-cell and cell-extracellular matrix (ECM) interaction. The brain microenvironment, including blood vessels, immune cells, inflammatory cells, signalling molecules, and matrix proteins, can affect tumour progression by interacting directly with cancer cells. Several attempts to recreate brain cancer tissue *in vitro* are described in literature. However, to date, it is still unclear which main characteristics the ideal model should reproduce. Thus, each research group starts from a different hypothesis obtaining completely different three-dimensional model. For all these reasons, the overall goal of this project was the development of a 3D *in vitro* model able to reproduce the brain ECM microenvironment and to recapitulate intrinsic physiological and pathological conditions for the study of tumor stroma interactions, tumor invasion ability, and molecular phenotype of glioma cells. Firstly, we performed an *in silico* bioinformatic analysis using GEPIA2 Software to compare the expression level of seven matrix protein in the LGG tumors with healthy tissues. The results showed that the most differentially and significantly overexpressed proteins between the tumor and healthy tissue are: Hyaluronic acid, Collagen IV, Fibronectin, Tenascin C and GFAP. Then, we carried out a FFPE retrospective study in order to evaluate the percentage of expression of five selected proteins in two districts of brain tissue (parenchyma and perivascular site). The proteins resulted to be differentially expressed in the different subtypes and between the two areas. Combining the results of the two different analyses, we developed a 3D scaffold composed by Hyaluronic Acid and Collagen IV in a ratio of 50:50. We evaluated that this platform was suitable for the cell culture. We used two astrocytoma cell lines, HTB-12 and HTB-

13. Firstly, we optimized the right seeding concentration using our 3D collagen I scaffold model already developed from our team. Subsequently, we evaluated the growth capability of the two cell lines on 3D neuro scaffold compared with 3D collagen I scaffold. We did not appreciate a significant difference in cell growth between the models. Instead, we assessed the high growth cell capability and the cell distribution on both 3D collagen and neuro scaffold by confocal microscopy, and we appreciated a significantly overexpression of various stemness markers by qRT-PCR in cells growth on 3D neuro scaffold. In order to better study the molecular and biological features of brain cancer, we optimized a protocol to isolate primary culture from surgical specimen from patients with LGG. Up to date, we obtained a stabilized primary culture from two of all the 14 specimens received. We performed a gene expression analysis by Real time PCR on these samples at different culture passages. Some genes correlated with aggressive and stemness features resulted to be overexpressed (MMP2, MMP9, VIM). The developed 3D neuro scaffold will be useful for the study of patients derived culture. In conclusion, we developed an *in vitro* three-dimensional brain model able to partially reproduce the composition of brain tumor extracellular matrix, demonstrating that it is a feasible platform to investigate the interaction between tumor cells and the surrounding matrix. The 3D neuro model is able to sustain the growth and proliferation of glioma cells and allow for different downstream analysis. This model will be implemented for the analysis of primary culture and tuned with different proteins ratio.

Introduction

1. Brain Tumors

Brain tumors account for 85% to 90% of all primary central nervous system (CNS) tumors. Worldwide, an estimated 308,102 people were diagnosed with a primary brain or spinal cord tumor in 2020[1]. In addition to primary brain tumors, there are also secondary brain tumors or brain metastases. The most common cancers that spread to the brain are breast, kidney, and lung cancers, as well as leukemia, lymphoma, and melanoma. Brain and other nervous system cancer is the 10th leading cause of death for men and women[1]. The 5-year survival rate for people in the United States with a cancerous brain or CNS tumor is almost 36%. The 10-year survival rate is almost 31%[1].

1.1 Classification and diagnoses

Gliomas are the most frequent primary malignant brain tumors in adults with an estimated annual incidence of 7.1/100,000 cases in the United States[2]. They can occur anywhere in the CNS, but primarily they are observed in the brain and arise in the glial tissue[3]. Glioblastoma (GBM) encounters 55% of all glioma diagnoses, while the remaining 45% of cases are represented by other glioma subtypes[2]. GBM is one of the most aggressive malignancies with a low median overall survival (OS), approximately only 15 months[4], while for the other glioma subtypes the median OS is 6.5-8 years[5,6]. The new World Health Organization (WHO) 2021 classification separated adult-type diffuse glioma from pediatric-type and associated the histopathological features with the molecular profiles and alterations to provide a more specific diagnosis[6]. The adult-type gliomas are mainly divided into isocitrate dehydrogenase (IDH) mutant and IDH wild-type (wt) tumors[7]. In the primary group, composed of IDH-mutated tumors, are included oligodendroglioma, presenting 1p/19q codeletion (grade 2/3) and astrocytoma, without 1p/19q codeletion (grade 2/3/4)[6,8]. The mutation in IDH1 and 2 genes are somatic, missense, heterozygous, and involved either codon R132 of IDH1 (> 90% cases) or codon R172 of IDH2 (<3% cases)[9,10]. Missense mutation in these two codons is associated with the glioma CpG island methylator phenotype (G-CIMP)[7]. The 90% of all IDH mutation affect the IDH1 R132H position, and it is possible to be diagnosed with an immunohistochemistry (IHC) assay[9]. In normal condition, IDH1 and 2 are homodimeric enzymes that catalyze the reversible decarboxylation of isocitrate to α-ketoglutarate (α-KG) with the production of NADPH, in the cytosol and peroxisomes through IDH1 or in the mitochondria with IDH2[10]. Under mutation condition, this conversion failed and the neomorphic activity of the mutant enzyme results in NADPH-dependent reduction of α-KG to the oncometabolite 2-hydroxtglutarate (2-HG)[10]. In IDH-mutated cells the concentration of 2-HG is >100-fold higher than in the normal cells. This oncometabolite induces a competitive suppression of several α-KG-dependent enzymes

involved in epigenetic regulation with a result of various epigenetic changes, such as histone and DNA hypermethylation[10]. In the second group, gliomas defined as IDH-wt, the presence of IDH-wt and other molecular alterations such as TERT (Telomerase Reverse Transcriptase) mutation, EGFR (Epidermal Growth Factor Receptor) amplification, or gain of chromosome 7/loss of chromosome 10 allows defining these tumors as a molecular GBM. Gliomas with H3K27 alterations (27th amino acid of Histone 3) are a new entity of IDH-wt gliomas diagnosed in pediatric patients but occasionally also in adults[2].

For the diagnosis of gliomas, there are different evaluations occurred with various techniques. Tumor tissue is formalin fixed and embedded in paraffin for histological and immunohistochemical staining as well as for molecular genetics and cytogenetic studies[7]. If possible, a tumor sample tissue should be cryopreserved for molecular assessments that require high-quality DNA and RNA samples. The diagnostic process should follow the WHO classification of 2021 and the subsequent recommendations from cIMPACT- NOW. Accordingly, glioma classification integrates histological tumor typing and grading as well as analyses of molecular markers (Fig.1)[7]. Next-generation sequencing-based gene panels could enable the assessment of all or most genetic and chromosomal aberrations relevant for diagnosis using a single assay. Array-based DNA methylation profiling has emerged as a powerful novel diagnostic method that is independent of histology and useful in the routine diagnostic workup[11]. Moreover, RNA sequencing-based approaches present a promising strategy for the detection of oncogenic gene fusions with diagnostic and/or predictive value that can be found in rare subsets of diffuse gliomas[7].

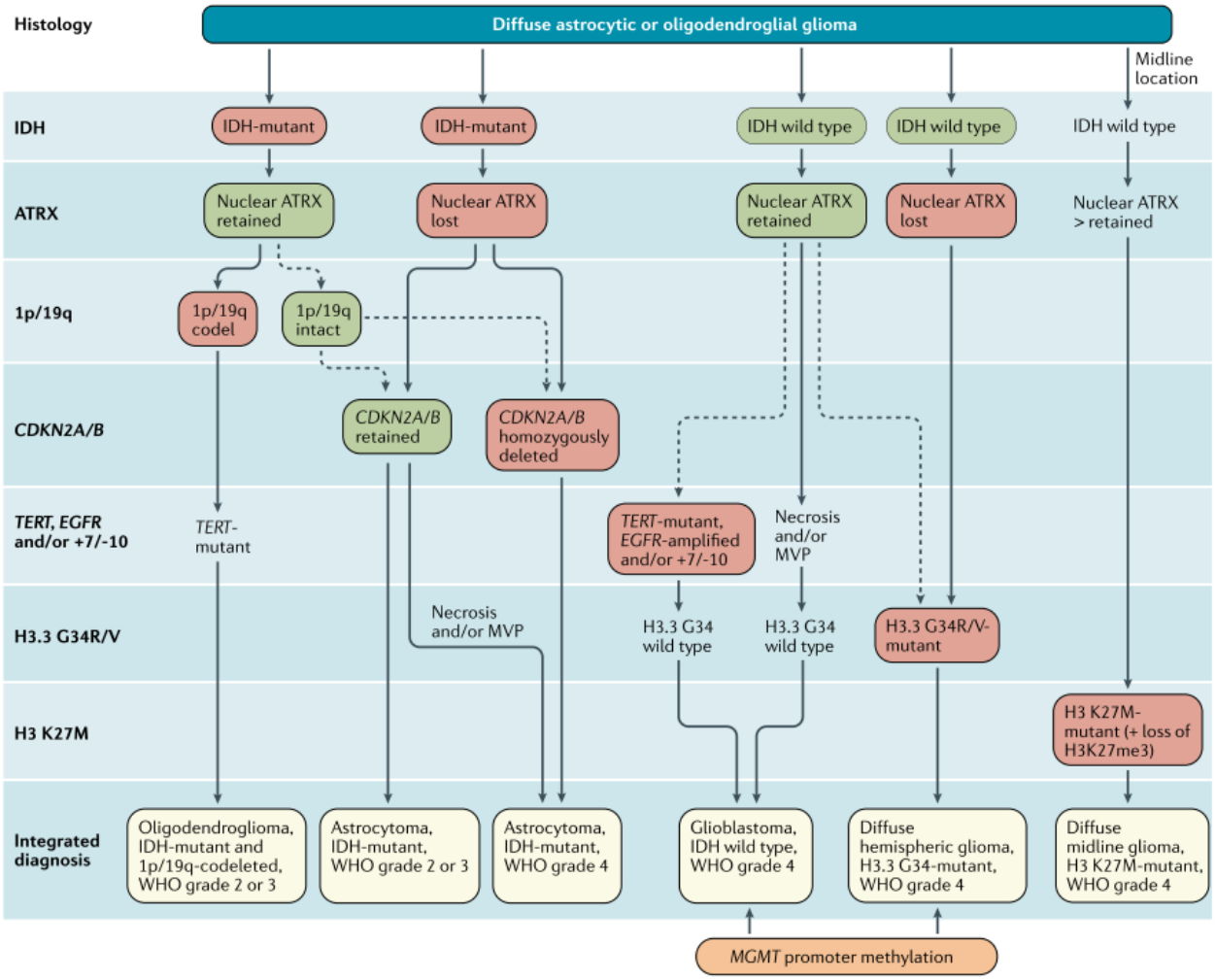

Fig.1 WHO 2021 *- Diagnostic algorithm for the integrated classification of the major diffuse gliomas in adults*[7].

1.2 Current Therapeutic Strategy

The main therapy-independent prognostic factors for the adult-type glioma are younger age and better performance status at diagnosis and are associated with favourable outcomes[7]. The IDH mutation status has a diagnostic value, but it is often associated with a relative favourable prognosis; also, the 1p/19q co-deletion has a diagnostic and prognostic value because of the prediction of response to alkylation chemotherapy[12]. But MGMT promoter methylation status is the most important prognostic factor[7].

Tumor resection is the most important step in the therapy of gliomas. The surgery has three major objectives: (1) obtaining tissue for the diagnosis; (2) improving the quality of life and overall survival (OS) and progression-free survival (PFS) by relieving focal deficits and improving seizure control; (3) remove as much tumor tissue as possible using microsurgical techniques, without the

compromission of neurological functions[7,9]. A lesser extent of resection and larger post-surgical residual tumor volumes are negative prognostic factor across gliomas of all grades and subtypes[7].

After the surgery, the radiotherapy is one of the possible strategies to manage glioma patients. In fact, this treatment wants to improve disease local control without inducing neurotoxicity. The timing, the dosing and the scheduling of radiotherapy are determined by the disease subtype and prognostic factors, as age, KPS (Karnofsky performance status), molecular factors, and residual tumor volume. Commonly, radiotherapy is administered at 50-60Gy in 1.8-2Gy daily fractions[7].

Most patients affected by glioma receive chemotherapy with alkylating agents. The most commonly used drug is Temozolomide, an oral DNA alkylating agent able to pass the blood-brain barrier (BBB). This treatment is frequently associated with radiotherapy in the STUPP regimen. Other alkylating agents used are fotemustine, carmustine, nimustine or lomustine drug; this last is often combined with procarbazine and vincristine in a regimen referred as PCV[7], that could be used after the radiotherapy regimen. The management of glioma patients derived from the subtype which they are affect. In the *Fig.2* are summarized the recommendation for IDH-mut and -wt gliomas treatment by WHO 2021[7].

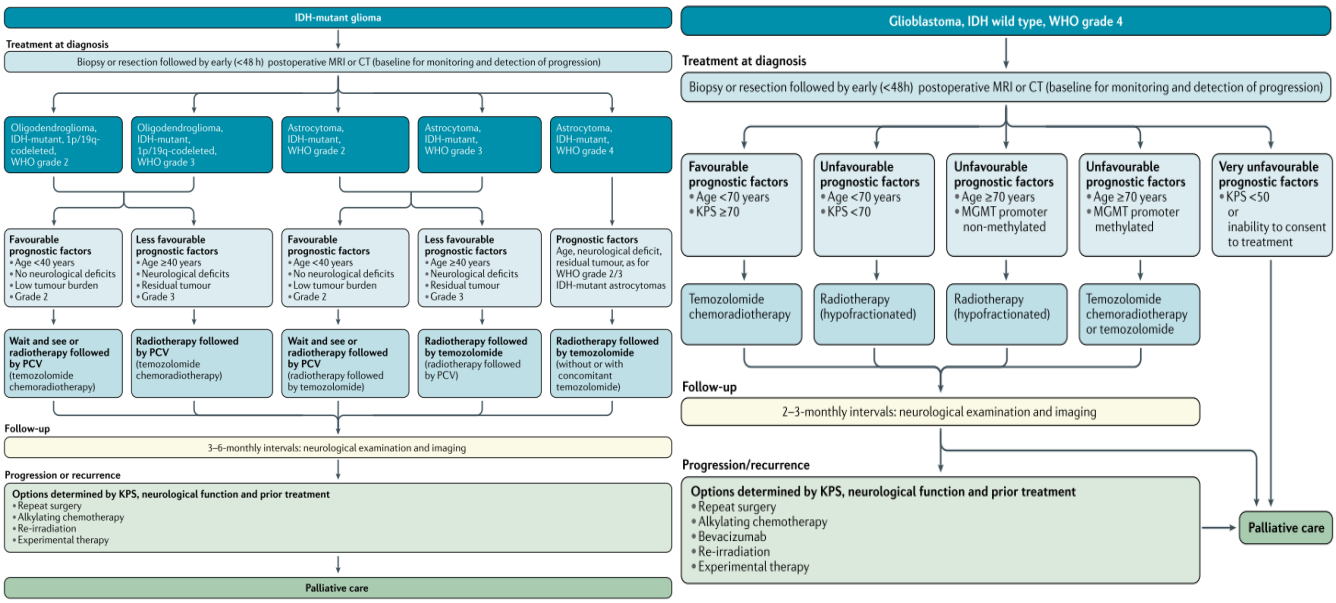

Fig. 2 *Recommendation for treatment of IDH-mut and -wt gliomas*[7].

2. *Brain Tumor Microenvironment*

In the last few years, important improvements toward a better understanding of genetic and epigenetic pathways regulating glioma development and growth have been done. These alterations differ in each glioma subtype explaining the different histology, clinical course, and biological behavior. Another key element influencing the development, progression, and clinical evolution of gliomas could be the tumor-associated microenvironment (TME)[2]. The brain TME, includes both malignant and non-malignant cells - tumor cells, blood vessels, a variety of infiltrating peripheral immune cells, inflammatory cells, signaling molecules, and the cells of the healthy brain such as neurons, neuroglia, and the additional components of the neurovascular unit (NVU), including pericytes and endothelial cells and the extracellular matrix, can regulate tumor progression by interacting directly with cancer cells[13–15]. Among the non-malignant cells are local immune cell types, such as microglia and astrocytes, as well as lymphocytes, endothelial, and other cells. Half of the tumor mass is composed of infiltrating cells, and most of the tumor-associated immune population are macrophages or microglia (*Fig.3*) [14].

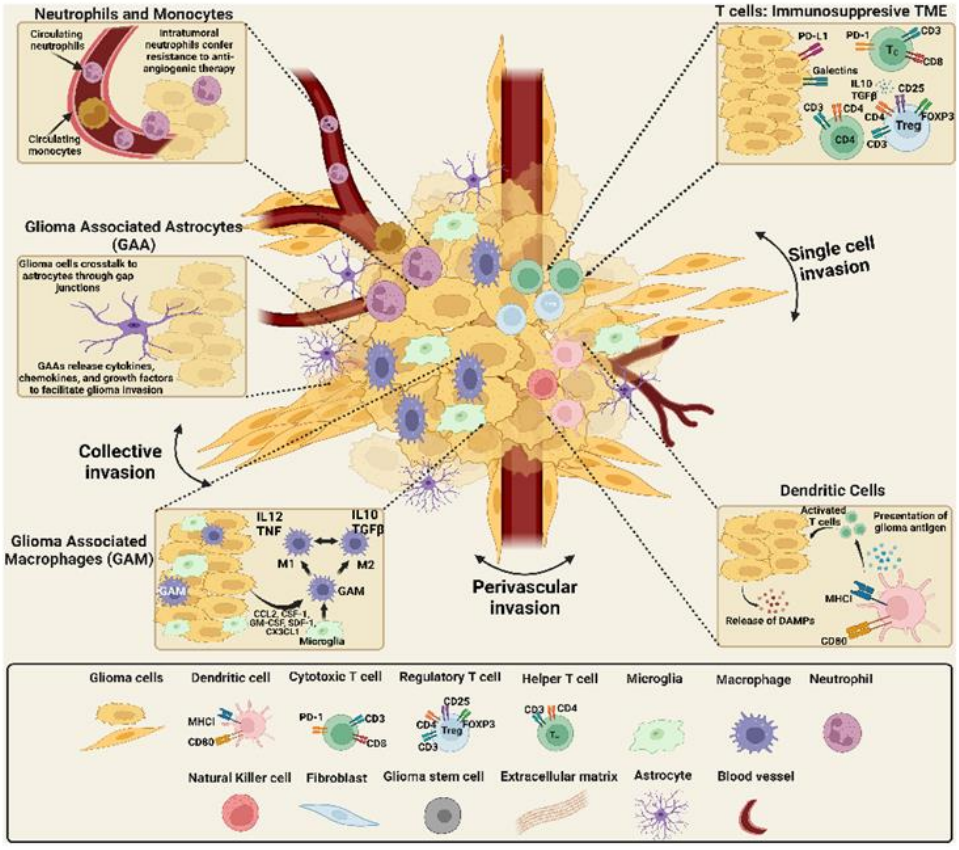

Fig.3 *Schematics of the cellular components of the brain tumor microenvironmental landscape. The cellular components of gliomas: malignant and non-malignant cells, including tumor cells, a range of invasive peripheral immune cells, cells from the healthy brain including neurons and neuroglia, as well as pericytes and endothelial cells*[14].

2.1 Extracellular matrix

The extracellular matrix (ECM) is a dynamic milieu that plays a pivotal role in the regulation of cellular functions during normal and pathological remodeling processes such as embryonic development, tissue repair, inflammation, tumor invasion, and metastasis[15]. Although the ECM contains mainly collagens and non-collagenous glycoproteins such as glycosaminoglycans and proteoglycans; its composition is probably unique for each cell type within an organ[16]. In brain tissue, neural ECM is a well-organized complex molecular structure surrounding neurons and glial cells[17]. The parenchyma of the central nervous system appears to be filled with a relatively amorphous matrix that contains mainly Hyaluronic Acid (HA) and little collagen and other fibrous proteins. A well-defined ECM exists in the form of a true basement membrane, cerebral vasculature, and glial limitans externa. The latter is a basement membrane that covers the brain's entire cortical surface and also, separates astrocyte foot processes from pial cells and the subarachnoid space. The basement membrane works as a regulator between endothelial cells and brain parenchymal cells[15]. The cerebral vascular basement membrane, which surrounds the blood vessels of the brain, contains type I, III, and IV collagens, fibronectin, laminin, and heparan sulfate proteoglycans[16]. The perineuronal net (PNN), characteristic of the neural cell surface, is a reticular network observed on the cell bodies and proximal dendrites[17]. HA constitutes the backbone of PNN, which binds to chondroitin sulphate proteoglycans. The high polarity of the proteoglycans attracts water molecules and creates a softer tissue, in contrast to more fibrous ECM[15]. The heterogeneity of proteoglycans in brain ECM is dependent on differential expression of genes encoding core proteins, alternative splicing and transcription-termination and variations in the length and types of glycosaminoglycan (GAG) side chains. The matrix's structure also includes lecticans, tenascin-C and tenascin-R[18]. The last component of the brain ECM structure is the interstitial matrix connecting the neurons and the vasculature (*Fig.4*)[15]. Neural ECM has distinctive biophysical properties, such as low elastic modulus and large porosity, as compared to other tissues, such as heart, cartilage, and bones. In particular, the elastic modulus of the brain tissue is approximately 110 Pa for neonatal and less than 1 kPa for adults. It is also known that matrix stiffness has a significant effect on neural cell behavior and morphology[15].

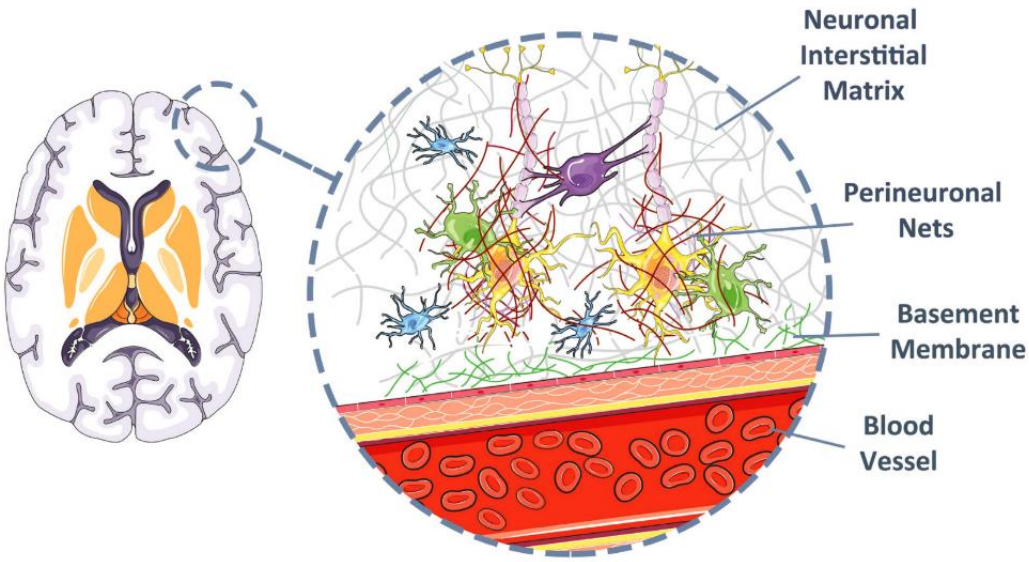

Fig. 4 *Cellular structure of the brain tissue*[15].

Extracellular Matrix Components

Proteoglycans

Proteoglycans and glycosaminoglycans (GAG) are abundantly present in the brain parenchyma and play a key role in the brain as growth factor reservoirs and stabilizers for ligand-mediated signaling by acting as co-receptors[19]. Proteoglycans, in particular chondroitin sulfate and heparan sulfate, have been found to induce cell motility[16]. Hyaluronic Acid (HA) is another essential component of the brain ECM and is the simplest glycosaminoglycan[20]. HA is a high molecular-weight proteoglycan found in the extracellular matrix, and it is the only proteoglycan that does not contain a core protein. It is formed by a negatively charged long polymer chains forming random coils intertwined in solution. HA is found in most extracellular matrices and at the cell surface. Elevated levels of HA have been correlated with brain tumor cell invasiveness[21]. HA interacts with other extracellular matrix proteins via hyaluronan binding proteins and receptors such as cluster differentiation 44 (CD44)[16] and the receptor for hyaluronan-mediated motility (RHAMM), which has a central role in glioma cell motility, invasion, and inflammation[22]. It has been demonstrated that high levels of CD44 are necessary to generate infiltrative glioma mouse models and that treatment with anti-CD44 antibodies inhibited tumor progression, possibly due to altered hyaluronic acid binding [14,23].

Fibronectin

Fibronectin is a glycoprotein found in most ECM, where formed an intricate fibrillar network connecting cells to the ECM[24]. Fibronectin is a dimer and multi-domain proteoglycan that is encoded by a single gene but has 20 isoforms via alternative splicing[25] and it is secreted by several cells including mesenchymal cells, fibroblast, endothelial cells, and perivascular smooth muscle cells which, in turn affects the proliferation, migration, and cell-adhesion of tumor cells[20]. Fibronectin is involved in many biological functions, as cell adhesion, migration, and invasion[16] and its expression correlates with tumor progression and prognosis as mediated by TGF-b signaling [14,26].

Tenascins

The Tenascin family comprises a large group of glycoproteins generated by alternative splicing resulting in different variants, including TN-C, TN-R, TN-W, TN-X, TN-Y. Tenascin is highly expressed during embryonic development, wound healing, and cancer [27,28]. Tenascins are large disulfide-linked heterodimeric extracellular glycoproteins. Tenascin-C (TN-C) is the original member of a family of heterodimeric extracellular matrix proteins, and it is implicated in adhesion and migration of human glioma cells. Tenascin binds to cell integrins, modifying cellular function, and also binds to other ECM molecules, such as brevican or neurocan, modifying cell migration and, focal adhesion. Moreover, Tenascins have been identified as an oncogenic molecule promoting glioma cell proliferation and inhibiting apoptosis in response to paclitaxel treatment via PI3K/AKT signaling regulation[14,29]. Tenascin-C is upregulated in most types of carcinomas, including malignant melanomas and gliomas[16].

Laminins

Laminin is a structural glycoprotein that is a part of a large group of adhesion glycoproteins found in all basement membranes with Collagen IV, Fibronectin and Perlecan and in hyperplastic blood vessels in gliomas and meningiomas. Laminin is a glycoprotein formed by three different chains, the a, b, and g chains, each encoded by different genes. It plays a role in migration, neurite outgrowth, proliferation, and differentiation[16,30]. Glioma tumors with higher expression of Laminin show accelerated cellular spread and tumor recurrence[14].

Type IV Collagen

Type IV Collagen, mainly present in capillaries and large blood vessels, is the principal collagenous constituent of most basement membranes[15]. Also, it is localized to the subendothelial basement membrane of blood vessels in gliomas[16].

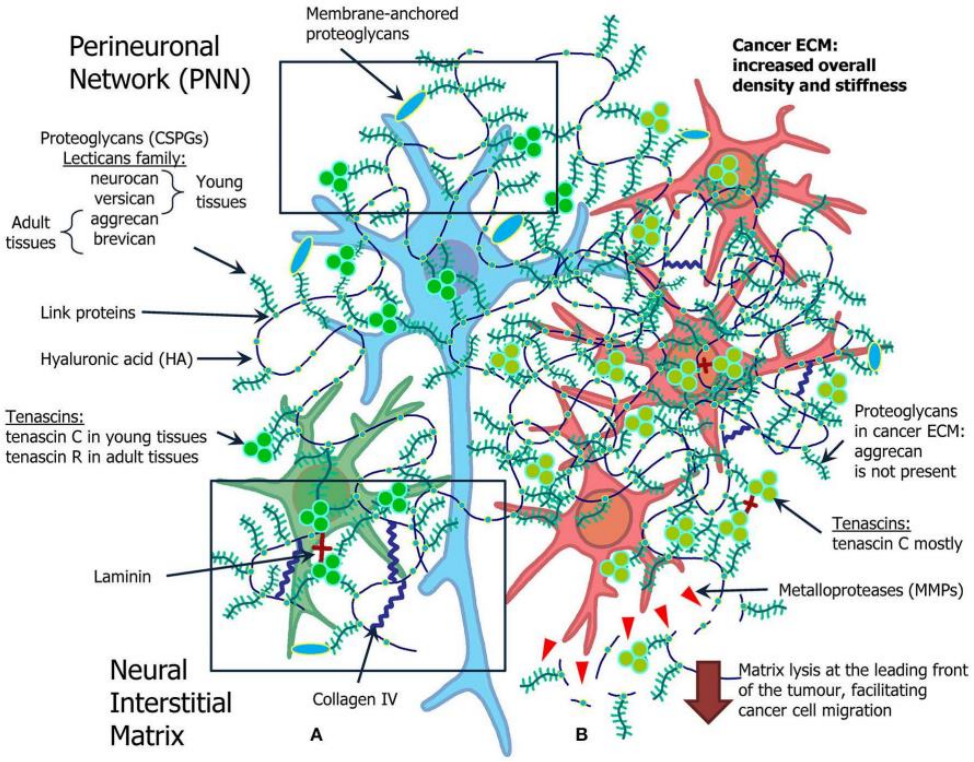

Fig.5 *Overview of the ECM in the normal brain (blue) and in brain tumors (red)*[31].

In literature, some authors assert that glioma ECM composition is critically different from that of normal brain (*Fig.5*), and that glioma tissue contains a large amount of fibrillar collagens, which are important ligands for the activation of signal transduction networks required for glioma malignancy[17]. Also, ECM plays an important role in glioma invasion. Some studies revealed alterations in the expression of specific ECM components in glioblastoma compared with that in non-tumor brain or astrocytomas grade 2 or 3 [32]. The ECM in astrocytoma differs from those of non-tumor brain both in quantity and in quality[33]. Various components of the ECM, such as cell-surface receptors and their ligands, ECM macromolecules, and enzymes have been shown to play a pivotal role in the invasion of cancer cells[33]. Virga et al. have analyzed the differences between mRNA expression level in non-tumor and low-grade astrocytoma. They found nine molecules differentially expressed: *CD44, HAS-1 and -2, Integrin-α1, Integrin-β1 and - β2, TGFβ1, TGFBI and TGIF-2*[33]. These molecules seem to play a specific role in the development of invasiveness of astrocytoma develops. CD44, as a receptor for HA, is a widespread component of tumor ECM and

has a pro-invasion role. HAS-1 and -2 enzymes, which synthetize HA, are also involved in increased astrocytoma motility and invasion. Probably, their function might be to hydrate the ECM by the excess amount of HA and, this loosening the structure of ECM and provide space for migrating cancer cells. Integrins are important in cell-ECM interaction and have a pro-invasive function. TGF-β and related TGFBI and TGIF2 are probably important in the epithelium-mesenchymal transition, and thus the invasion[33]. In another study of Virga group, it was identified that two HA's receptors, CD44 and CD168, are significantly increased in GBM compared to normal tissue[34].

2.2 Three-dimensional models

3D *in vitro* neural models have recently received significant ever-growing attention. The modern neuroscience mainstream increasingly relies on 3D models to study neural circuitry, neural regeneration, and diseases. Functional 3D neural tissue models can provide insight into brain development, exploration of new therapeutic solutions, and cost-effective drug discovery investigations[15]. In the long term, 3D *in vitro* neural models will potentially represent the human neural system better and can be used more often in regenerative medicine[15].

Understanding the cell-level hierarchy of the brain tissue is an important step toward developing a successful model of the brain tissue[35]. The cell type diversity, mechanical properties of the surrounding environment, and the chemical interactions between the cells and the environment together represent a complex living matrix[15]. 3D models, derived partially or completely from patient tissue or incorporating biomaterials, are a new technology that has risen as a potential tool to better recapitulate TME dynamics[36].

Every cell in the human body is immersed in a 3D microenvironment that regulates its behavior and potentially, its fate[36]. In this setting, *in vitro* models aiming to understand glioma biology in order to develop effective therapies should ideally mimic the TME[36]. Traditional two-dimensional (2D) cell culture system is commonly used, and it is the most accessible for *in vitro* modeling[36,37]. Also, the 2D system is often used to assess the sensitivity of tumor cells to radiotherapy and chemotherapy and guides the clinical treatments[38]. Unfortunately, the 2D approach presents various limitations such as (1) does not accurately reproduce tissue architecture[38], (2) the introduction of genetic and epigenetic modifications due to the lack of cell-ECM interactions[37,39], (3) absence of O2, nutrients and pH microenvironment gradients, (4) lack of physiological inputs from other metabolically active organs such as liver, kidney, etc., (5) genomic alterations after long-term culture, reducing the similarity to *in vivo* primary tumors[36,37,40], and (6) presents deviations in drug sensitivities between *in vitro* tests and *in vivo* clinical evaluations[38]. *In vitro* models, recapitulating native tumor-

stromal interactions and cell-ECM interactions of cancer cells in a reproducible, efficient, and high-throughput manner, may serve as better alternatives to *in vivo* models[37]. 3D structures enable the formation of tissue-mimetic architectures and promote more realistic physiological responses than conventional 2D cultures, through recreating cell–cell and cell–ECM interactions[41]. *In vitro* 3D models in glioma cancer research can be classified in spherical cancer models, organoids, and 3D scaffolds[36].

Spherical cancer models

Spherical cancer models consist of sphere-like structures mainly or totally composed of cancer cells[42]. In this section are included the tumorspheres or neurospheres. Thanks to their easy production, they are the most commonly used 3D *in vitro* model. They derived from the proliferation of single-cell suspension of tissue-derived cancer cells, circulating cancer cells, or established cell lines (clonal expansion)[36]. Tumorspheres are able to maintain cancer stem cells multipotency, resemble 3D interactions, and reproduce the tumor gradient of oxygen and nutrients. Thus, they present a quiescent necrotic core and a more proliferative outer layer[36]. Tumor spheroids can be grown in suspension in the regular specific stem cell media or submerged in a gel, which has allowed them to be used as an important tool for high-throughput drug screening[43]. These 3D tumor models are found to recapitulate 3D cell-cell interactions and transport properties, thus promoting *in vivo*-like tumor behavior[40]. For example, glioma spheroids more closely recapitulate the molecular profile of the parental tumor and present more stable molecular aspect over time[44] and mimicking *in vivo* drug sensitivity compared to 2D cultures[40].

Organoids

Organoids are 3D *in vitro* models with improved biomimicry compared to other *in vitro* culture methods[45]. They are self-organizing, 3D microscopic structures that are derived from individual stem cells growing in an *in vitro* environment, and they can recapitulate histoarchitecture and cellular composition, as well as physiological aspects of the mature primary tissue they are derived from[36]. Organoid fabrication protocols have been developed, but the variability among organoids and the limited control of cellular organization within organoids due to the self-assembly process limit their broader applications[45]. In literature, there are a lot of examples of organoids, especially developed for GBM studies. Hubert et al. developed GBM organoids to better maintain the cellular heterogeneity and the gene expression of primary tumors, and the tumor cells within organoids display enhanced hypoxic state and stemness compared to their counterparts 2D cultures[45]. Organoids have a higher order of assembly due to the presence of a special matrix (e.g., Matrigel) and spatial cues, which leads to the formation of organ-like structures[15].

3D scaffolds

Scaffolds are 3D materials that provide support and structure to cell cultures; these biomaterials have microscale mechanical properties such as stiffness, porosity, interconnectivity, and structural integrity that can modulate cellular behavior[46]. In general, these properties as well as structural patterns, textures, and composition can be controlled in the attempt to recapitulate ECM characteristics proper to the specific tissue of interest[36]. Because of the glioma TME possesses a distinct ECM composition with a high proportion of fibrillary collagens when compared to normal brain parenchyma, 3D glioma cultures using 3D collagen scaffolds have been studied with interest. Different scaffolds created with other relevant tumor ECM components such as HA as well as with synthetic materials are also described[47]. The use of 3D biomaterials used to simulate ECM mechanical properties and cell–ECM interactions has led to a deeper understanding of the mechanobiology underlying tumor malignancy, cancer cell migrations, and resistance to therapies[36]. The biomaterials used to establish 3D culture system include poly (lactic-co-glycolic) acid, chitosan, alginate, Matrigel and collagen[38]. The commonly applied biomaterials in studies of glioma are Matrigel and hydrogel, and their application is mainly focused on the detection of the sensitivities of co-cultured tumor cells to radiation and drugs[38]. Therefore, researchers have investigated the use of 3D scaffolds to create an artificial structure that can mimic the *in vivo* tumor microenvironment, which could be used as a platform for more representative *in vitro* study and screening of therapeutics. These 3D structures provide a more reliable tumor model for *in vitro* trials due to the arrangement of cancer cells in a 3D structure with increased cell-cell and cell-extracellular matrix (ECM) signaling[48]. The preparation of 3D porous scaffolds with chemical composition resembling native tumor microenvironment ECM could further enhance the malignancy of cultured cancer cells and provide a more predictive analysis of drug[48–50].

Another new field for 3D model is the 3D bioprinting process, that can generate well-defined structures in all three dimensions, with high resolution, reproducibility, flexibility, and customizability[37]. Biomimetic 3D models require biomaterials with good biocompatibility and tissue-specific properties, including appropriate biophysical/biochemical properties and degradation kinetics[37]. The major bioprinting methods include inkjet-based, extrusion-based, and light-assisted bioprinting processes. Biomaterials form structural networks that foster cell adhesion, proliferation, and migration, and provide specific spatiotemporal cues to modulate cell behaviors[37].

Aim of the project

Last decade research has seen impressive progress in understanding the fundamental aspects of glioma biology in terms of genetic factors, intra-tumor heterogeneity, differential behaviors of glioma stem cells, and changes in their growth and invasion actions. Nevertheless, these efforts have not offered a significant benefit to patients[51]. Several attempts to recreate brain cancer tissue *in vitro* are described in literature; however, to date, it is still unclear which main characteristics the ideal model should reproduce. Thus, each research group starts from a different hypothesis obtaining completely different three-dimensional model. The different devices are composed with different matrix proteins and compounds including collagen-based scaffold, matrigel and hydrogel supports, chitosan hyaluronic acid scaffolds, and bioprinting models. Although brain-ECM receptors/ligands have increasingly been characterized, brain-ECM studies in general have been difficult, in part, due to the lack of access to specific fresh matrix components for *in vitro* testing[52]. These systems overcome some monolayer and organoid limitations, but they don't completely reflect the brain ECM structure and composition. Moreover, there is more research focused on models able to recapitulate glioblastoma structure compared to the other subtypes, due to their rarity. For these reasons, the overall goal of this project was the development of a 3D *in vitro* model able to reproduce the brain ECM composition of glioma and to recapitulate intrinsic physiological and pathological conditions for the study of tumor stroma interactions, tumor invasion ability, and molecular phenotype. The synthesis and development of a new 3D model started from a retrospective study focused on the identification of the ECM composition in the different subtypes of low-grade glioma patients. This system will be useful for a better understanding of the mechanisms involved in the crosstalk between tumor and ECM. The resulting model, mimicking the glioma ECM and *in vivo* tumor growth, will enable a deeply investigation of the molecular mechanisms involved in the natural history of gliomas. Development of this new device will improve the preclinical research on gliomas enabling the study of cancer cells behaviour and drug efficacy in an environment that better mimic the *in vivo* cancer microenvironment.

Materials and Methods

Bioinformatic Analysis

The ECM proteins expression profiles were evaluated using GEPIA2 Software (Gene Expression Profiling Interactive Analysis), which comprises the TCGA/GTEx public clinical dataset for different cancer subtypes. LGG cancer subtype was selected, and the tumor biomarker value of each selected target was investigated by differential expression analysis between normal and tumor tissue. Moreover, we performed a correlation analysis between protein expression level and patients Overall- and Disease-free survival to confirm the prognostic value for each marker analyzed.

Retrospective patient study: immunohistochemical analysis

Thanks to the collaboration with the Pathology Unit of Ospedale Bufalini (Cesena) we performed a retrospective study. Matrix protein expression levels were evaluated in formalin fixed embedded primary tissues of 25 cancer patients. Patients aged ≥18 years with histologically confirmed diagnoses of Astrocytoma grade 2 and 3, Meningioma or Oligodendroglioma grade 2. Selected glioma patient's FFPE embedded tissue were tested by Immunohistochemical (IHC) staining to evaluate the ECM proteins composition and their relative concentrations. Different protocols specific for each antibody were used. The analysis was performed on the Ventana platform. The following proteins were detected: Collagen IV, Fibronectin, Laminin, Tenascin C, GFAP.

Scaffold synthesis

All chemicals necessary for scaffold synthesis were purchased from Sigma Aldrich (St. Louis, MO, USA). Collagen scaffolds were synthesized as followed: a 1wt% suspension of type I collagen in acetic acid was prepared and precipitated to pH 5.5. The material was cross-linked through a 1wt% 1, 4-butanediol diglycidyl eter (BDDGE) to stabilize the collagen matrix and to control porosity and tortuosity. Scaffold's porosity and pore size was obtained through an optimized freeze-drying process, consisting of an established freezing and heating ramp (from 25 °C to −25 °C and from −25 °C to 25 °C in 50min under vacuum conditions, p=0.20 mbar), ultimately ensuring proper pore interconnectivity and orientation.

For 3D Neuro scaffolds, human Collagen IV, and Hyaluronic Acid (from Sigma Aldrich - St. Louis, MO, USA) solution was mixed and cross-linked as previously described in a ratio of 50:50 in order to mimic the tumor brain matrix.

All scaffolds were sterilized by immersion in 70% ethanol for 1hour, followed by 3 washes in sterile Dulbecco Phosphate Buffered Saline (DPBS) (Life Technologies, Carlsbad, CA, USA).

Cell seeding and culture

The experiments were performed on two human Astrocytoma cancer cell lines, HTB-12 and HTB-13, obtained from the America Type Culture Collection (Rockville, Maryland, USA). All cells were maintained in ATCC-formulated Leibovitz's L-15 Medium supplemented with 10% fetal bovine serum, 1% penicillin-streptomycin (PAA, Piscataway, NJ, USA) at 37 °C in a 5% CO2 atmosphere. For standard cultures, $1\times10^{\wedge6}$ cells were maintained as a monolayer in 25-cm2 flasks in 4 ml of culture media. For 3D cultures, each scaffold (1×6mm) was placed in a 12-multiwell plate and seeded with $0.2\times10^{\wedge6}$ cells by adding 15 µl of cell suspension on the scaffold upper surface. Seeding was reached by simple soaking of the cell suspension in the dry scaffolds. Cells were incubated for 1 hour at 37°C to allow adhesion, after that 4 ml of culture medium were carefully added.

MTT assay

Briefly, cells within the scaffolds or in monolayer cultures were incubated with 0.5 mg/ml of MTT solution (Sigma Aldrich) in PBS for 2 hours at 37 °C. The metabolically active cells reduced MTT to blue formazan crystals. After 2 hours, MTT-formazan crystals were dissolved in isopropanol and hydrochloric acid (HCl) and the absorbance was determined at 550 nm on a Synergy H1 Biotek (Agilent).

PrestoBlue assay

The PrestoBlue (PB) assay is a commercially available, ready-to-use, water-soluble preparation. Cells viability assay with PB reagent was performed according to the manufacturer's protocol. The cells within the scaffolds or in monolayer cultures were incubated with PB reagent. The changes in cell viability were detected using fluorescence spectroscopy. The fluorescence was recorded at excitation 540 nm and emission 610 nm from 1h-incubation to 4h-incubation of cells with PB reagent. To ensure that PrestoBlue was not toxic to human cancer cells and that it did not affect the measurements (especially, after longer incubation times), the cells incubated with or without PrestoBlue, were examined for cell viability using MTT assay, as described above. After, the timepoint of 3 hours-incubation was selected for the following analysis.

Hematoxylin and Eosin staining

3D collagen and neuro scaffolds were dehydrated by incubation in increasing concentrations of ethanol (50–100%), embedded in paraffin, sliced with a rotating microtome (Leica Biosystems) at 5 µM thickness and mounted to Superfrost Plus microslides (Thermo Fisher Scientific). Haematoxylin and Eosin staining (H/E) was performed to evaluate scaffold architecture, cell morphology and distribution.

Immunofluorescence Staining

For immunofluorescence staining, cells seeded in 3D collagen scaffolds and in 3D neuro scaffolds were fixed 20 min in 4% PFA at room temperature and then blocked to minimize unspecific binding of the antibody and permeabilized with PBS + 1%BSA+0.3% Triton X-100. DAPI staining was used to counterstain the nucleus whereas Phalloidin Staining (Alexa Fluor™ Phalloidin) was used to detect filamentous actin (F-actin). Images were imaged by A1 laser confocal microscope (Nikon Corporation, Tokyo, Japan) and analyzed with the NIS Elements software (Nikon Corporation, Tokyo, Japan).

Quantitative real-time reverse transcriptional-PCR (qRT-PCR)

The scaffolds were fragmented into small pieces, while 2D culture cells were collected by trypsinization. Total mRNA was isolated using TRIzol Reagent (Invitrogen) following the manufacturer's instructions. Five hundred nanograms of RNA were reverse-transcribed using the iScript cDNA Synthesis Kit (BioRad, Hercules, CA, USA). The final mixture was incubated at 25 °C for 5 min, at 42 °C for 20 min, at 47 °C for 20 min, at 50 °C for 15 min and 5 min at 85 °C. Real-Time PCR was performed on the 7500 Real-Time PCR System (Applied Biosystems, Foster City, CA, USA) using the TaqMan gene expression assay mix (Applied Biosystems). Amplification was performed in a final volume of 20 µl containing 2x Gene expression master Mix (Applied Biosystems), 2 µl of cDNA in a total volume of 20 µl. The reaction mixtures were all subjected to 2 min at 50 °C, 10 min at 95 °C followed by 40 PCR cycles at 95 °C for 15 sec and 60 °C for 1 min for overall markers. The stably expressed endogenous HPRT was used as reference gene. The following markers were analyzed: matrix metalloproteinase-2 (MMP2) and matrix metallopeptidase 9 (MMP9), Vimentin (VIM), NOTCH1 and CD44. The amount of transcripts was normalized to the endogenous reference gene and expressed as n-fold mRNA levels relative to a calibrator using a comparative threshold cycle (Ct) value method (ΔΔCt). For the analysis, the calibrator used was the RNA extracted from naive surgical specimen for the qRT-PCR of the primary cultures, while for the cell lines the calibrator used was the time point collected at 24h.

Establishment of primary cultures

Tumor tissues received in sterile carrier medium were processed immediately. Briefly, tumor tissue was minced by scalpel and digested with Collagenase I for 30 minutes at 37°C with intermittent shaking. After passing through a cell strainer, the single cell suspension was seeded in T25 culture flask and on 3D collagen scaffold in NeuroCult™ Neural Cell Culture complete Media (STEMCELL™ Technologies).

Results

In silico study

In literature, there are many different studies designed to develop and characterize a model of brain tumor microenvironment. It is well-known that the correlation between cell and matrix plays a pivotal role in the tumor development and growth. Thus, we performed a bioinformatic analysis using the GEPIA2 Software (Gene Expression Profiling Interactive Analysis), which comprises the TCGA/GTEx public clinical dataset: we compare seven proteins, which are present in the brain matrix, to identify which ones were overexpressed in the LGG tumors (N=518 specimens) compared to the healthy tissues (N=207 specimens). The results showed that between the tumor tissue (in red) and the healthy tissue (in black) the most differentially and significantly expressed proteins are: Hyaluronic acid, Collagen IV, Fibronectin, Tenascin C and GFAP (*Fig.6*).

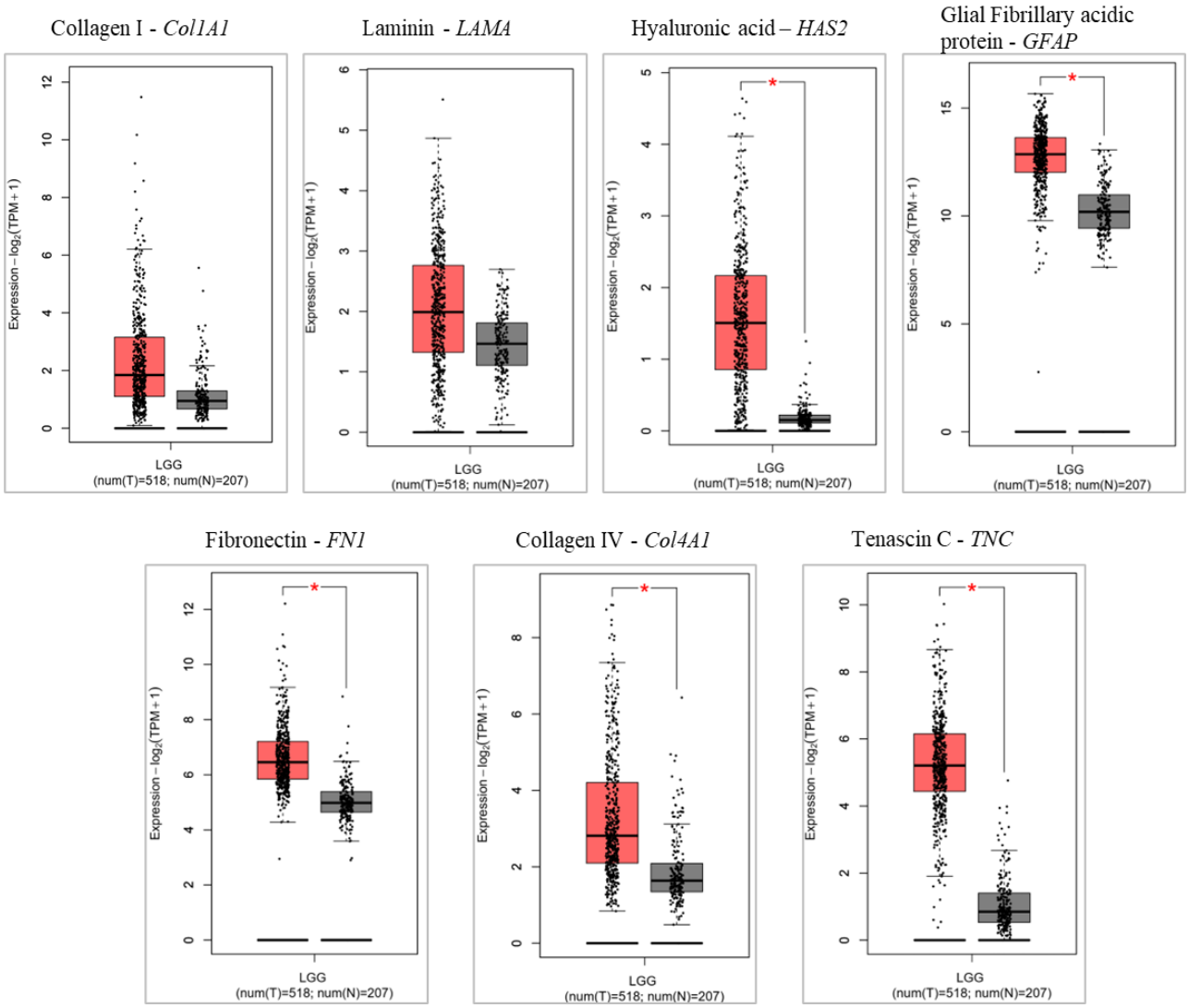

Fig. 6 *Proteins expression profiles in low grade glioma tumors (red) compared to healthy tissue (black). Analysis was performed with bioinformatics analysis using GEPIA2 Software, which comprises the TCGA/GTEx public clinical dataset. Statistical analysis was performed using Student's t-test, *p<0.05*

The dataset did not allow the analysis of protein expression value according to different LGG subtypes. However, it was useful to evaluate correlation between protein expression and patient's clinical outcome (overall survival-OS and disease-free survival-DFS).

A higher expression of the five proteins that emerged as overexpressed in glioma was also found to correlate significantly with a worst prognosis in terms of OS and DFS (*Fig.7*).

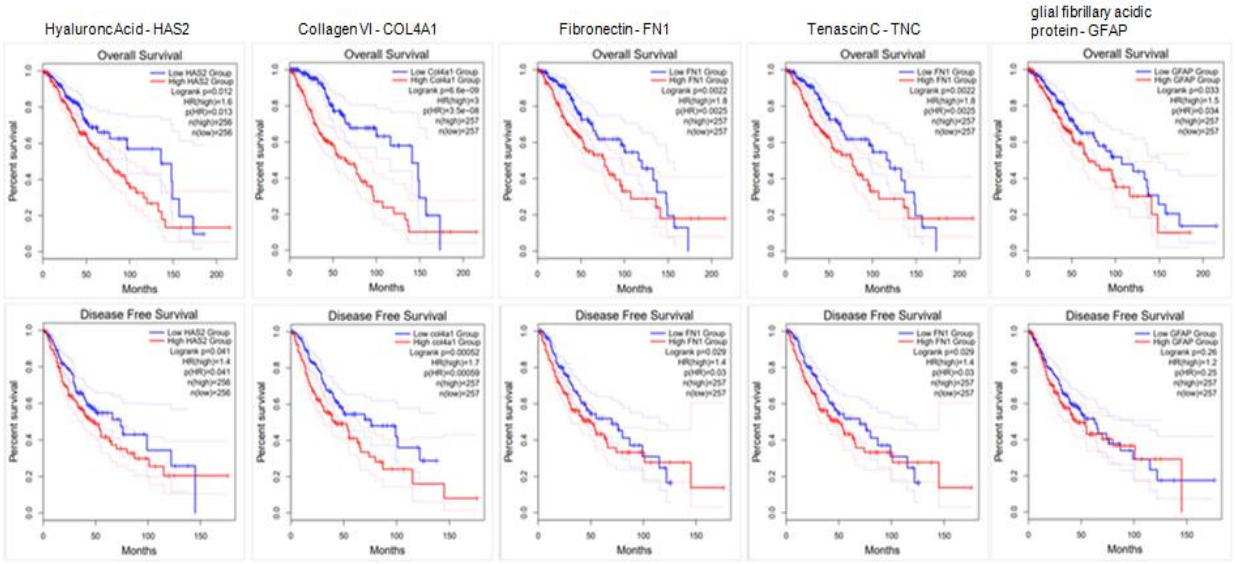

Fig.7 *Kaplan-Meier of Overall survival (OS) and Disease-free survival (DFS) of patients with high (red) or low (blue) expression of 5 different proteins: Hyaluronic acid, Collagen IV, Fibronectin, Tenascin-C and GFAP.*

Retrospective study on FFPE embedded patients' tissue

Thanks to the collaboration with the Pathology Unit of Ospedale Bufalini (Cesena), we enrolled 25 patients for the FFPE retrospective study. On these samples, the pathologist carried out the immunohistochemical analysis on five of the seven proteins, selected as above mentioned by *in silico* analyses. Patients were stratified as follows: 8 meningiomas, 10 astrocytomas and 7 oligodendrogliomas with different grade (1-3). The pathologist evaluated the expression of the different proteins in two districts of the tissue: parenchyma and vascular site. Data were scored from 0 to 3, based on the expression value of the protein, in the analyzed slice. The data were shown below in Table 1. The retrospective study was performed before the WHO 2021, so the diagnosis reported in Table 1 was accorded with WHO 2016.

PARENCHYMA					
Diagnosis	GFAP	COLLAGEN IV	LAMININ	FIBRONECTIN	TENASCIN-C
Meningothelial Meningioma I	0	0	0	1	0
Fibrous Meningioma I	0	3	0	0	0
Meningioma grade I	0	1	0	0	3
Atypical Meningioma II	0	2	2	2	0
Atypical Meningioma II	0	2	2	2	0
Atypical Meningioma II	0	1	0	2	0
Atypical Meningioma II	0	1	0	2	1
Anaplastic Meningioma III	0	0	2	1	1
Diffuse Astrocytoma II	3	0	0	0	0
Diffuse Astrocytoma II	3	0	0	1	0
Diffuse Astrocytoma II	3	0	0	0	0
Diffuse Astrocytoma II	3	0	0	3	0
Diffuse Astrocytoma II	3	0	0	1	0
Diffuse Astrocytoma II	3	0	0	1	0
Diffuse Astrocytoma II	3	0	0	0	1
Anaplastic Astrocytoma III	3	0	0	0	2
Anaplastic Astrocytoma III	3	0	0	1	0
Anaplastic Astrocytoma III	3	0	0	0	2
Oligo II	3	0	0	1	0
Oligo II	3	0	3	3	0
Oligo II	3	3	0	0	3
Anaplastic Oligo III	3	1	1	3	1
Oligo-astrocytoma	3	0	0	1	0
Oligo II-III	3	0	0	0	0
Anaplastic Oligo III	3	0	0	1	0

VASCULAR					
Diagnosis	GFAP	COLLAGEN IV	LAMININ	FIBRONECTIN	TENASCIN-C
Meningothelial Meningioma I	0	3	2	2	0
Fibrous Meningioma I	0	3	0	0	0
Meningioma grade I	0	3	3	3	0
Atypical Meningioma II	0	3	3	1	0
Atypical Meningioma II	0	3	3	2	0
Atypical Meningioma II	0	3	3	0	0
Atypical Meningioma II	0	3	2	3	0
Anaplastic Meningioma III	0	3	3	3	0
Diffuse Astrocytoma II	3	3	3	3	0
Diffuse Astrocytoma II	3	1	1	0	0
Diffuse Astrocytoma II	3	2	1	0	0
Diffuse Astrocytoma II	3	0	3	0	0
Diffuse Astrocytoma II	3	3	3	3	0
Diffuse Astrocytoma II	3	3	2	3	0
Diffuse Astrocytoma II	3	3	2	3	2
Anaplastic Astrocytoma III	3	3	2	3	0
Anaplastic Astrocytoma III	3	2	1	1	0
Anaplastic Astrocytoma III	3	2	0	0	0
Oligo II	3	3	2	0	0
Oligo II	3	3	3	0	0
Oligo II	3	3	2	3	0
Anaplastic Oligo III	3	3	0	0	0
Oligo-astrocytoma	3	3	1	0	0
Oligo II-III	3	3	1	0	0
Anaplastic Oligo III	3	3	0	3	0

Table 1. ***Immunohistochemical analysis*** *on 25 FFPE embedded tissue of LGG patients for the 5 proteins analysed: GFAP, Collagen IV, Laminin, Fibronectin, Tenascin-C. Analysis was performed by the pathologist on two different sites of tissue: parenchyma and vascular site. Expression data was scored from 0 (no expression) to 3 (high expression)*

In order to assess the protein expression, related to the different subtype, in parenchyma and perivascular area, we performed the analysis through this operation:

$$\% = \frac{\text{n° patients score}}{\text{tot patient subtype}}$$

As a result, we obtained a different expression percentage for each protein, showed in Fig.8.

This analysis showed that GFAP was the most expressed protein, in both parenchyma and perivascular area, in astrocytoma and oligodendroglioma subtypes, differently it is not expressed in meningiomas. Conversely, Collagen IV is mainly expressed in meningioma subtype in both areas, whereas this marker was expressed only in the perivascular area in the astrocytomas and oligodendrogliomas. Despite the subtype, perivascular area tested positive for Laminin, at different degree of intensity, whereas tumor parenchyma was negative in 83% of all cases. Fibronectin is expressed in tumor parenchyma in about 70% of patients at low-moderate degree of intensity; the perivascular area was positive in 50% of patients. Tenascin-C was almost entirely absent in the vascular and perivascular area, while it was low expressed in the parenchyma of all the subtypes.

Fig.8 *Graphical results of the expression percentage in vascular and parenchyma site of the 5 proteins, related to each subtype.*

Synthesis of 3D neuro scaffold

Previously, we developed and characterized a Type I Collagen 3D scaffold as a suitable platform to model *in vitro* some of the key features of primary tumor growth and drug response[53]. As collagen I is not one of the main brain ECM proteins, according to the results obtained by the *in silico* analysis and the retrospective study, we decided to mimic brain ECM by developing a scaffold composed by two proteins: Hyaluronic Acid and Collagen IV. We decided to use a ratio of 50:50 of these two proteins. The 3D neuro scaffold was obtained with the same synthesis protocol. The two scaffolds are shown in Fig.9. The scaffolds have a dimension of 6 mm of diameter. For the experimental procedure, we cut the scaffold in slices of about 1-2 mm of thickness.

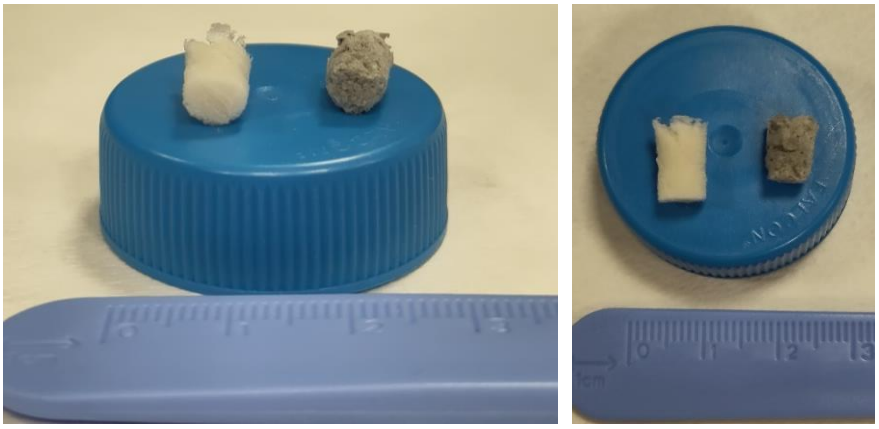

Fig.9 *Type I Collagen scaffold (white, on the left) – Neuro scaffold (grey, on the right)*

Characterization of culture condition

To obtain the ideal cell seeding concentration on 3D neuro scaffold, we performed a study of metabolic profile of two different cell lines, starting with 3D collagen I scaffold, our control condition. After the sterilization of the collagen scaffolds, we seeded the 2 cell lines, HTB-12 and HTB-13, on the scaffold at three concentrations: 0.1-0.2-0.5x10^6 cells/scaffold in a seeding volume of 15µL of cells suspension. We performed MTT assay in order to evaluate the metabolic capacity of the cell lines at different timepoint: 24-72 hours and 7 days after seeding. We compared the proliferation rate of cells seeded in 2D condition versus 3D scaffold condition (*Fig.10*).

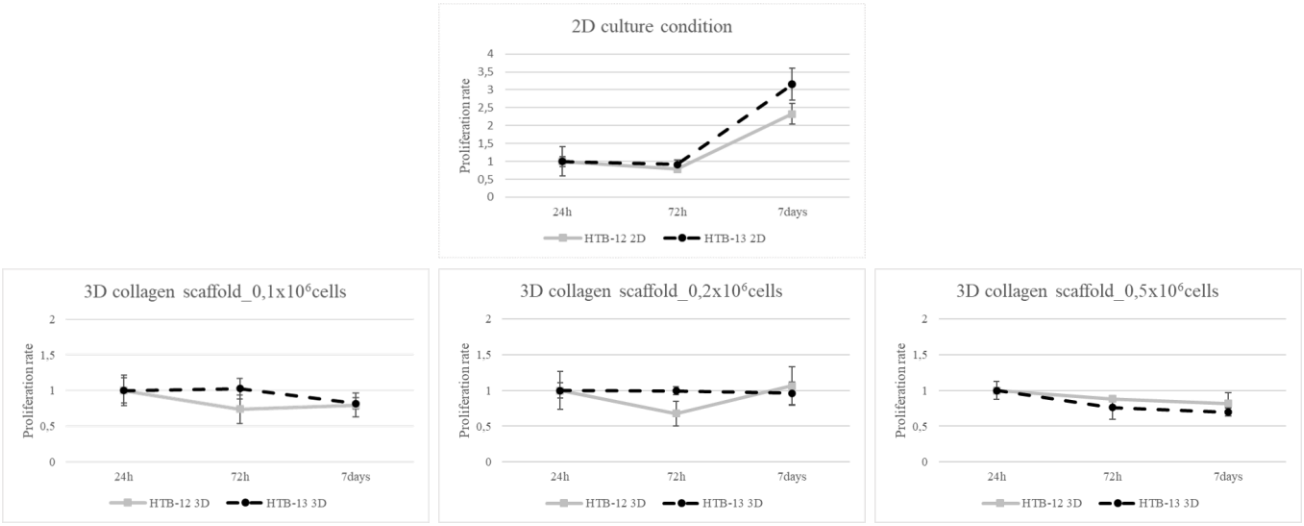

Fig.10 MTT Assay. *Proliferation curves of cell lines HTB-12 (grey) and HTB-13 (black) in 2D or 3D culture condition at three different timepoint: 24-72 hours and 7 days after seeding. On top the proliferation curve of 2D growth. below from left to right, the proliferation curve on 3D condition at the 3 different cell seeding concentration: 0.1-0.2-0.5x10^6 cells/scaffold. Data are presented as mean ± sd.*

We reproduce the same experiment, evaluating the proliferation rate with PrestoBlue assay (*Fig.11*). In this setting, we could use less scaffolds than MTT assay, because PrestoBlue analysis is transient, and it is a live assay.

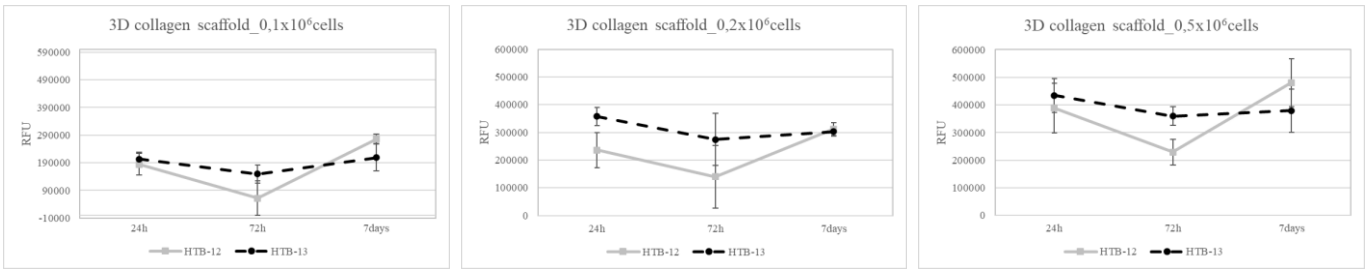

Fig.11 PrestoBlue Assay. *Proliferation curves of cell lines HTB-12 (grey) and HTB-13 (black) in 3D culture condition at three different timepoint: 24-72 hours and 7 days after seeding. From left to right, the proliferation curve on 3D condition at the 3 different cell seeding concentration: 0.1-0.2-0.5x10^6 cells/scaffold.*

Comparing the two assays, the HTB-13 cell line (*Fig.10-11* black dotted lines) showed a slower metabolic profile in 3D compared to the growth in 2D condition. Instead, HTB-12 cell line (*Fig.10-11* grey lines) showed a decreased profile at 72hours in all the 3 cells concentrations, but an increased metabolism at 7 days in the PB assay, while in the MTT assay this increase was not appreciated. These results highlighted the 0. 2x10^6 cells/scaffold as the most suitable cell seeding concentration.

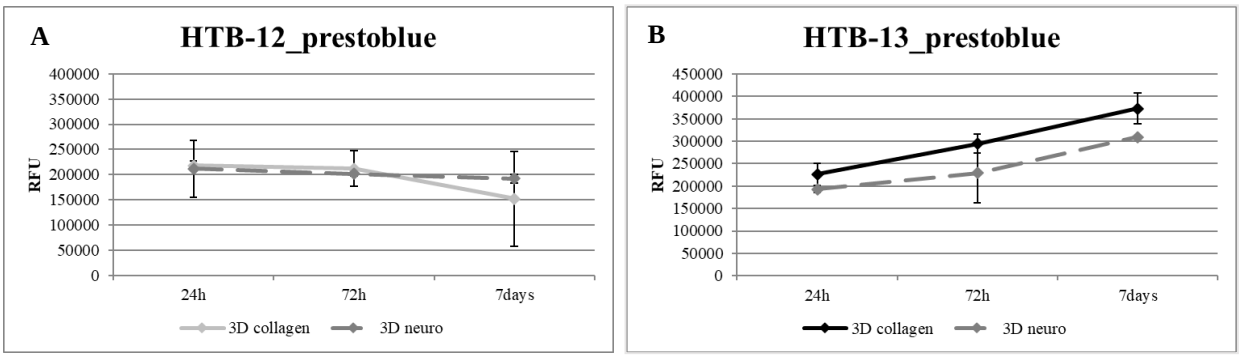

Fig.12 PrestoBlue assay*. Proliferation curves of cell lines HTB-12 (A) and HTB-13 (B) in 3D culture condition at three different timepoint: 24-72 hours and 7 days after seeding on 2 different 3D model: 3D collagen scaffold (continuous line) and 3D neuro scaffold (dotted line). Cell seeding concentration: 0.2x10^6 cells/scaffold.*

Then, we evaluated the growth capability of the two cell lines on 3D neuro scaffold. We performed a test to compare the proliferation curves of HTB-12 and HTB-13 seeded on 3D collagen scaffold versus 3D neuro scaffold. We used the concentration established with the previously experiments. The evaluation was made through PrestoBlue assay.

In Fig.12A, the PrestoBlue assay result of HTB-12 cell line growth in 3D condition at the seeding concentration of 0.2x10^6 cells/scaffold were shown. It is possible to appreciate a different proliferation rate compared to the same condition in Fig.11. It is also possible to notice, at the timepoint of 7 days after seeding, that the cells growth on 3D collagen scaffold had a decrease respect to the growth on 3D neuro scaffold, even if this trend was not significant. Instead, in Fig.12B, HTB-13 cell line had the same proliferation curve trend in the two 3D culture conditions. The differences were not significant.

The evaluation of the HTB-12 and HTB-13 growth capability and cell distribution throughout the scaffold was performed also by confocal microscopy. The cell lines grown on 3D collagen scaffold and 3D neuro scaffold were stained as previously described. In Fig. 13, representative pictures of 3D collagen scaffold (B-D) and 3D neuro scaffold (A-C) after 7 days of HTB-12 and HTB-13 seeding were shown. Cells were stained with Phalloidin Alexa Fluor-594 (red) and DAPI (blue). The acquisitions were made in large image, that is an image 5x5millimetre with a variable Z range; with a 20X lens and with a 40X lens with a variable Z range. From the images reported in Fig.13, it is possible to appreciate the colonization of both cell lines in both the 3D scaffold models. Cells did not show apoptotic nuclei or signs of suffering. HTB-12 cell lines shown a more spiral growth, probably in the pores of the scaffold, while HTB-13 cell lines shown a high proliferation and colonization in both the 3D scaffolds, as seen through PrestoBlue assay. There were differences between the two side of the scaffolds, indeed more cells colonized the seeding side respect to the other side. We will next analyse the expression of migration markers.

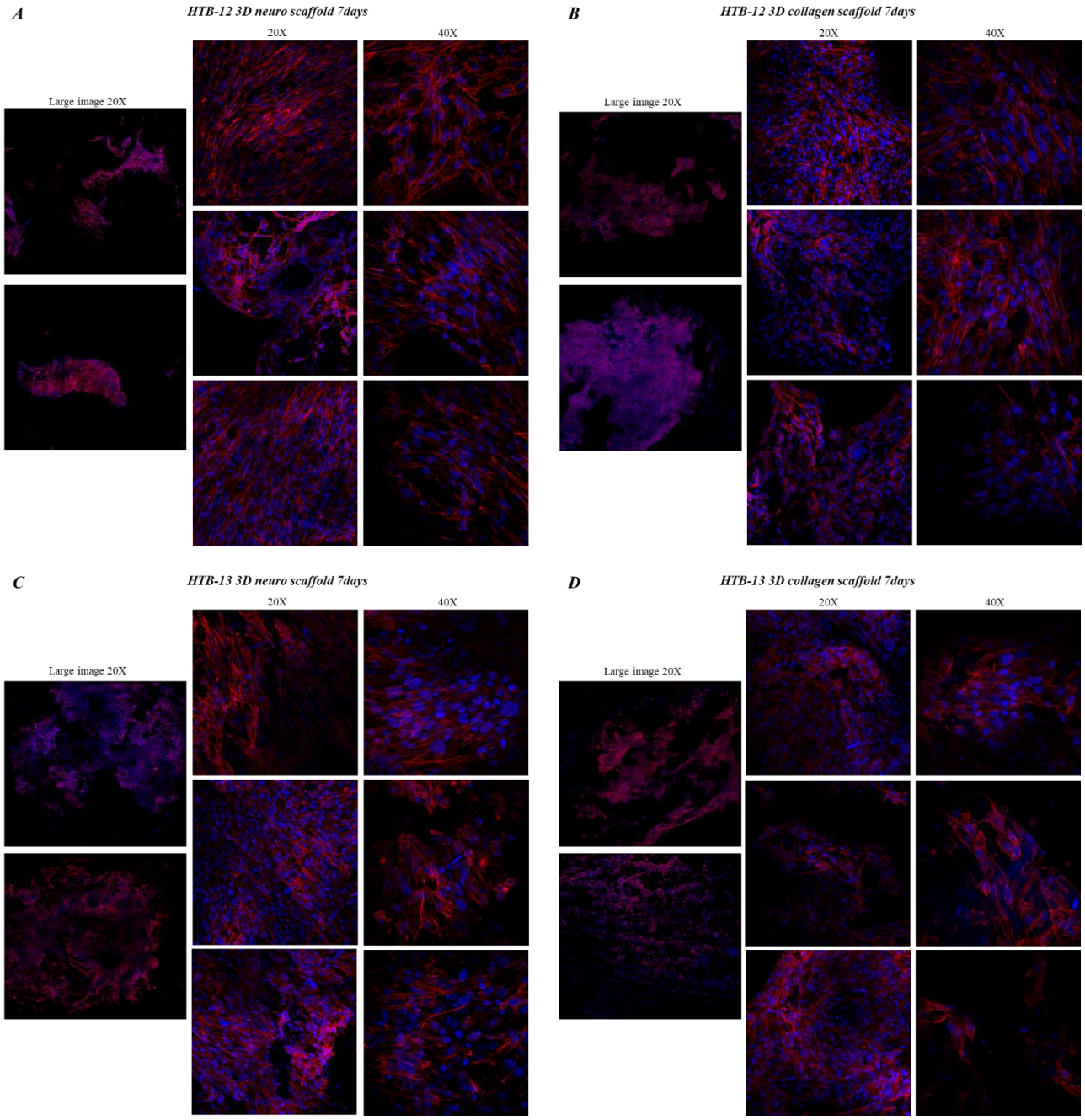

Fig.13 Confocal microscopy acquisition. *The cells were stained with Phalloidin Alexa Fluor-594 (red)to stain actin filaments (cytoskeleton) and DAPI to counterstain the nuclei (blue) (A-B) HTB-12 cell line seeded on 3D neuro scaffold and 3D collagen scaffold respectively. (C-D) HTB-13 cell line seeded on 3D neuro scaffold and 3D collagen scaffold respectively. The acquisitions were made after 7 days of growth.*

For both cell lines seeded on 3D neuro and collagen scaffold, we also performed a gene expression analysis by qRT-PCR (*Fig.14)*. We examined the expression of five genes correlated with aggressive and stemness features: matrix metalloproteinase-2 and -9 (MMP2-MMP9), Vimentin (VIM), Notch Receptor 1 (NOTCH1) and CD44, and their modulation during the 3D culture (24-72h-7days after seeding). The cell lines gene expression was normalized to the respective 24h specimen.

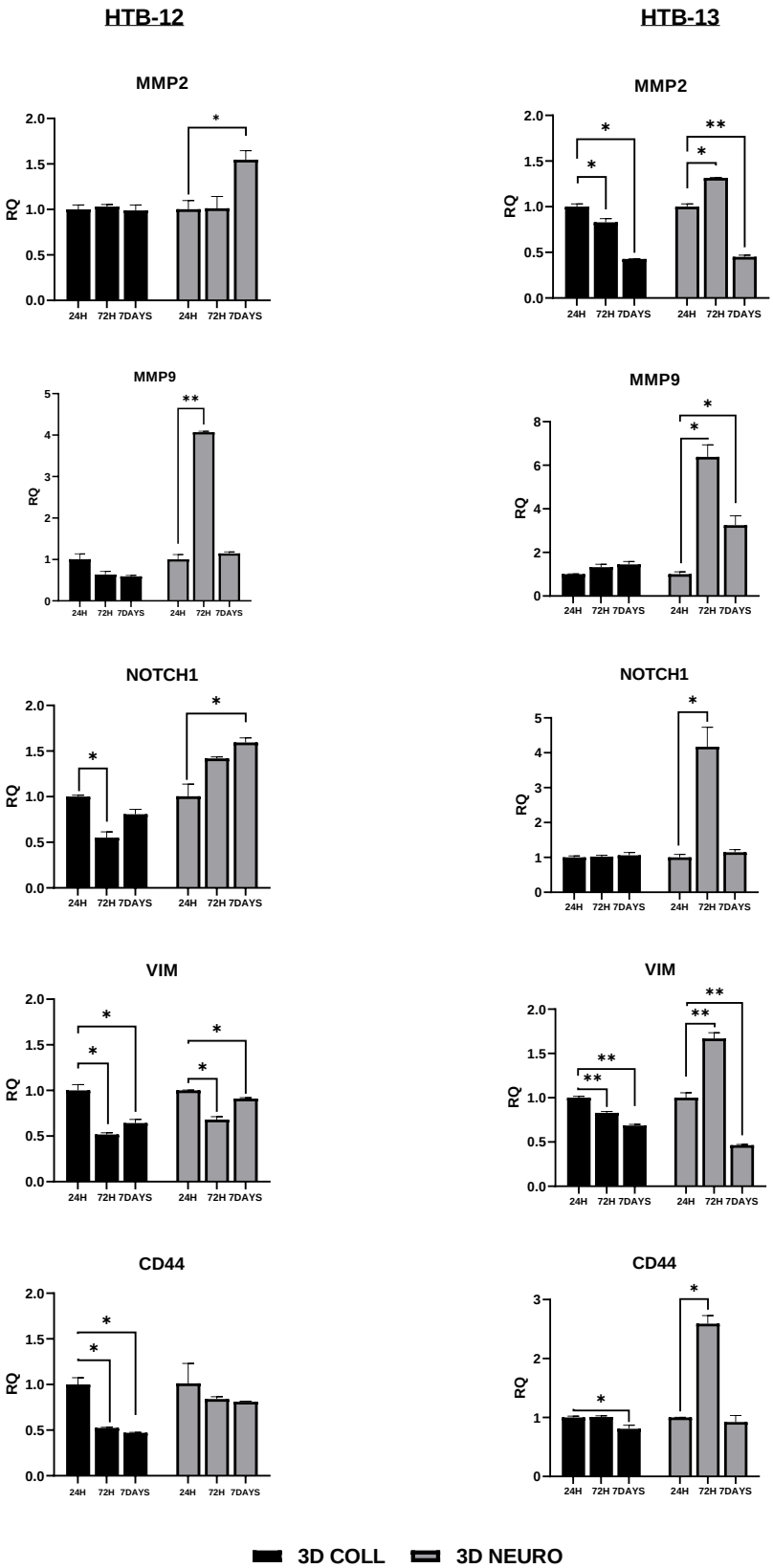

Fig.14 RT–qPCR. *Analysis of markers related aggressive and stemness features (MMP2, MMP9, VIM, NOTCH1, CD44) in HTB-12 (left) and HTB-13 (right) cells in 3D culture condition (Collagen-black; Neuro-grey) at different timepoints. Data were normalized on respective 24h specimen and represented as mean ± sd.*
**P < 0.05, two-tailed Student's t-test.*

In HTB-13 cell line growth on 3D neuro scaffold it is possible to appreciate at 72h timepoint a significant upregulation of all the five genes analyzed. Instead, on 3D collagen scaffold, the gene modulation was different: there was a significant downregulation of MMP2 and VIM, while NOTCH1 and CD44 expression didn't change. For HTB-12 cell line the results were different and only MMP9 gene was significantly upregulated at 72h timepoint, in the 3D neuro sample. For VIM target the results obtained for both 3D collagen and 3D neuro samples were similar.

Primary cultures

Thanks to the collaboration with the departments of Neurosurgery and Pathology Unit of Ospedale Bufalini (Cesena), we obtained 14 surgical specimens from patients with LGG. We optimized the protocol to isolate primary cultures from these specimens. For all the patients, we collected serum and plasma samples for the future NGS analysis. A part of the surgical sample was stored for subsequent molecular analysis, while the remaining sample was digested with mechanical and enzymatic procedures to obtain a stabilized primary culture (*Fig.15A*). We encoded the LGG samples with a progressive number. We considered a cell line stabilized when it reached at least the seventh passage. Up to now, we obtained a stabilized primary culture from two of all the specimens received (LGG4, LGG5). Fig.15 B-C showed the morphological features of LGG4 and LGG5 primary culture growth in 2D conditions. For LGG4 and LGG5, we studied not only the 2D culture, but also the 3D culture on collagen scaffold at two different time point: t0, cells seeded after surgical specimen digestion, and t7 or 9, when we considered the primary culture stabilized. The scaffolds were included in paraffin and Haematoxylin and Eosin staining was performed to visualize the cells morphology and distribution (*Fig.15B-C*).

For both stabilized primary cultures, we also performed a gene expression analysis by Real Time PCR. We examined the expression of four genes correlated with aggressive and stemness features: matrix metalloproteinase-2 and -9 (MMP2-MMP9), Vimentin (VIM) and Notch Receptor 1 (NOTCH1). The stabilized culture's gene expression was normalized to the respective surgical specimen. For the LGG4, the overexpression of MMP2 and VIM in the stabilized culture respect to the surgical specimen was statistically significant. Instead, in LGG5 there was an overexpression of MMP2, MMP9 and NOTCH1 but not for VIM. (*Fig.16*)

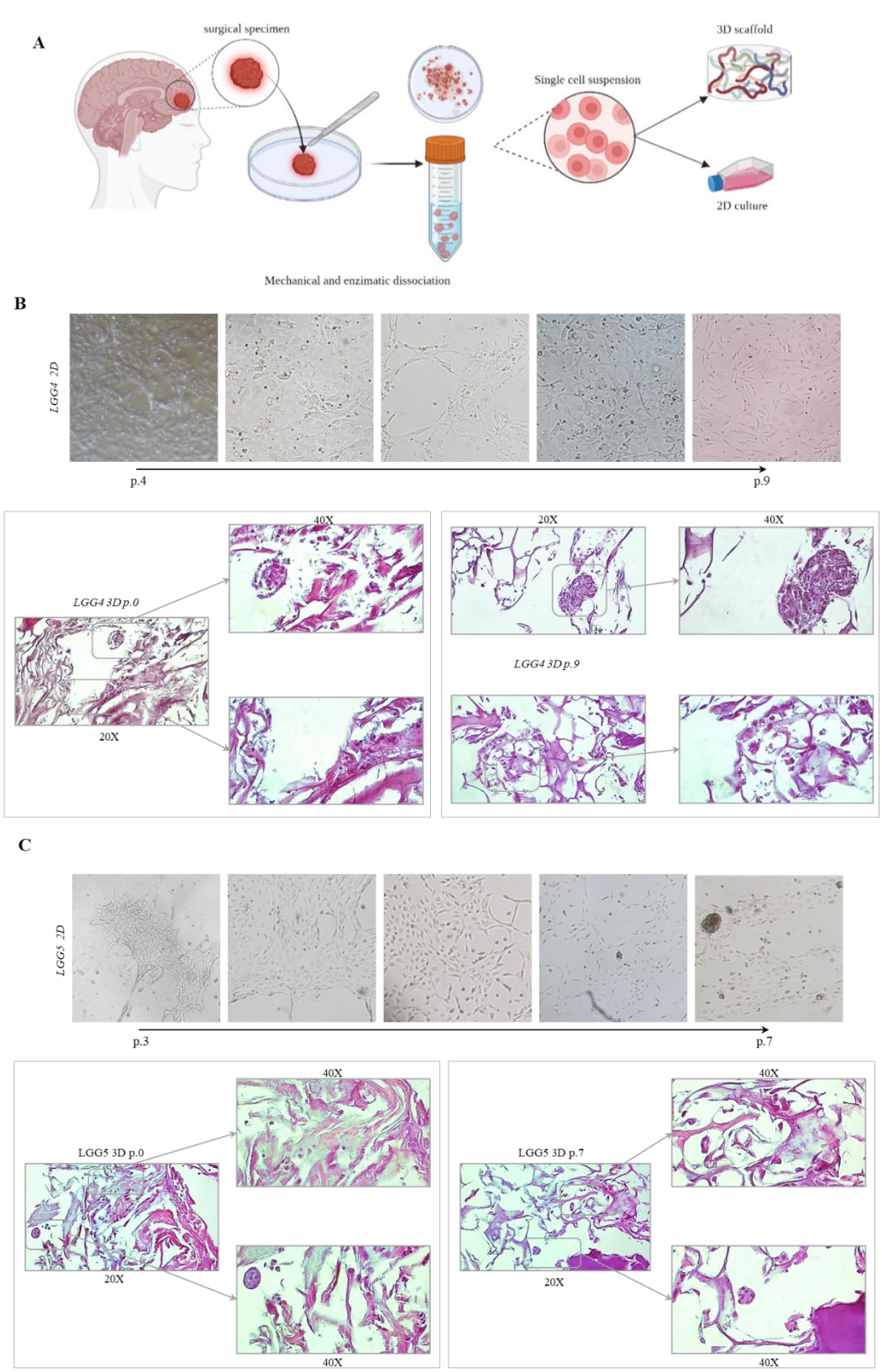

Fig.15 Primary cultures. A*. Graphical abstract of isolation protocol of primary culture from patient's surgical specimen (from Biorender.com).* ***B****. LGG4 primary culture. Photo of 2D culture from passage 4 to passage 9 and H&E staining on FFPE embedded 3D collagen scaffold at passage 0 and passage 9.* ***C****. LGG5 primary culture. Photo of 2D culture from passage 3 to passage 7 and H&E staining on FFPE embedded 3D collagen scaffold at passage 0 and passage 7.*

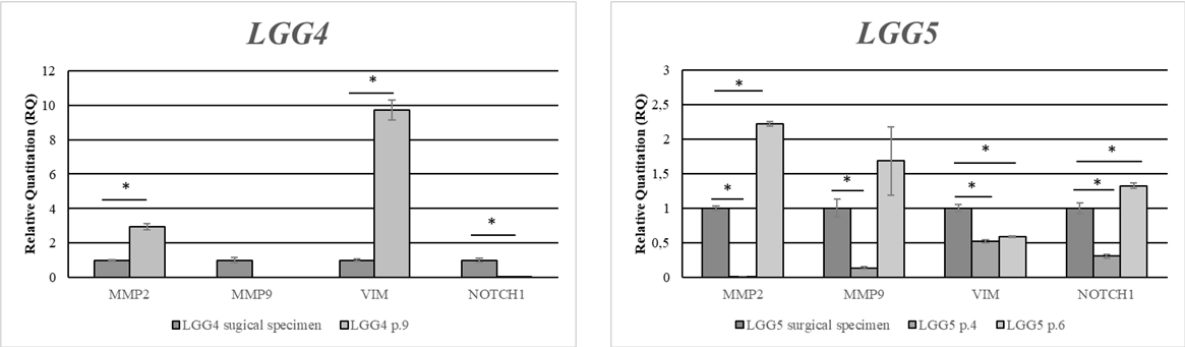

Fig.16 RT–qPCR. *Analysis of markers related aggressive and stemness features (MMP2, MMP9, VIM, NOTCH1) in LGG4 and LGG5 cells in 2D culture condition at different passage. Data were normalized on surgical specimen and represented as mean ± sd.*
**P < 0.05, two-tailed Student's t-test.*

Discussion

Brain and other nervous system cancer are the 10th leading cause of death for men and women[1]. In particular, gliomas are the most frequent primary malignant brain tumors in adults with an estimated incidence of 7.1/100,000 cases every year in the United States[2]. In the last years, the research tried to understand the role of the tumor-associated microenvironment (TME) as an important element influencing the development, progression, and clinical evolution of gliomas[2]. The brain TME, including blood vessels, immune cells, inflammatory cells, signaling molecules, and the extracellular matrix, can regulate tumor progression by interacting directly with cancer cells[13]. In literature, there are evidence that the brain extracellular matrix plays a pivotal role in the spread and progression of tumor. Many steps forward have been made, but a common idea of a brain model for the study of tumor cell-matrix interaction has not yet been reached. Two-dimensional models (2D) are a useful and feasible way to study the molecular characteristic of brain cancer cells, but it lacks key features related to microenvironmental context of the tumor, such as the hypoxic core. Hence, in this project, we aimed to develop a three-dimensional *in vitro* model able to mimic more closely the brain tumor extracellular matrix. With a step-by-step project, we aimed to recapitulate intrinsic physiological and pathological conditions for the study of tumor stroma interactions tissue, the tumor invasion ability, and the molecular phenotype of glioma cells.

In literature, there are lots of studies that attempt to describe the composition and variation of tumor microenvironment, but they focused mainly on the immunological counterpart. This actor is one of the most important, especially for the development of new treatment or for the use of novel drugs to treat brain cancer patients. Here, out data highlight that the tumor stroma and the extracellular matrix play a pivotal role in tumor progression. We started from an *in silico* study to understand the matrix proteins composition in brain ECM. In particular, we evaluated whether there were

differences between tumor and normal tissue in the protein's expression. Thanks to the GEPIA2 public clinical dataset, we confirmed five of the seven proteins analyzed as highly differentially expressed in tumor tissue, respect to healthy tissue. Some of these results confirmed the data obtained from literature, such as the role and the overexpression of Hyaluronic Acid. However, some of these proteins were not yet tested. These significant different proteins expression between healthy and tumor tissue could highlight their role in the tumor progression. Our FFPE retrospective study has allowed a step forward to better understand the spatial expression of the selected proteins in the tumor stroma. In accordance with literature data, we confirmed the overexpression of GFAP in all the cases of astrocytoma and oligodendroglioma and the complete absence in the meningioma cases. However, the expression level of the other proteins was not as expected, because of the lack of information in literature. From the obtained results, we decided to use four proteins: Hyaluronic Acid, Collagen IV, Laminin, and Fibronectin. For the synthesis of the 3D model, we started with Hyaluronic Acid, the most representative protein in brain parenchyma, and Collagen IV, for the architecture of the scaffold. The developed 3D neuro scaffold was stiffer than we expected. We used a ratio 50:50 of HA:Collagen IV, but we will try to use a different ratio, because, in our previous studies, we demonstrated that the stiffness can affect cancer cells behavior and aggressiveness[54]. We performed the 3D culture conditions starting from our previously established collagen I scaffold. We tested three different concentrations in order to evaluate which cell concentration was the most suitable for the growth and the maintenance of cellular phenotype. Based on our results, we selected the seeding concentration of $0.2x10^6$cells/scaffold, since cell lines did not present a growth decrease after 72 hours. The two metabolic assays data, MTT and PrestoBlue, did not reflect completely the analysis performed by confocal microscopy, especially for the HTB-12 cell line. This cell lines appeared organized, well distributed throughout the space, and in some area with a spiral growth, probably in the pores of the scaffold, both for 3D collagen and 3D neuro scaffolds. HTB-13 cell line presented a higher growth profile from the metabolic assays confirmed by the confocal analysis. Nuclei did not present any sign of apoptosis; on the contrary, they appeared bigger than we expected, which suggest the acquisition of a more aggressive phenotype. Cells grew along the scaffold fibres, and they presented a more elongated shape compared to the 2D culture condition. The data obtained by qRT-PCR on HTB-13 cell line seeded on 3D neuro scaffold reflected the aggressive phenotype observed by confocal microscopy. There was a significant upregulation of five genes (MMP2-MMP9-VIM-NOTCH1-CD44) correlated with aggressive and stemness phenotype, respect to the same cell line growth on 3D collagen scaffold. These results could suggest that 3D neuro scaffold can induce a modulation of aggressiveness and stemness pathways, maybe by providing a microenvironment more similar to

the *in vivo* ECM. Other markers will be explored to more deeply assess which are the neuro-ECM determinants of our scaffold able to affect the cell lines features. The establishment of primary culture from surgical specimen of LGG patients was a very important step in our project, because LGG are rare tumors and there are few commercially cell lines. We developed a protocol to obtain primary cultures which can be seeded on 3D neuro scaffold to maintain their aggressiveness and stemness features. Moreover, we confirmed the translational value of our previously 3D collagen scaffold. However, we will next evaluate how and why it affects the tumor growth differently compared to our 3D neuro scaffold. We studied the molecular profiles of 2D culture primary cell lines, and we appreciated a statistically significant overexpression of Vimentin and MMP2 and MMP9 genes in the established cell lines compared to the surgical specimen. Since these are mesenchymal and aggressiveness markers, this data suggested that we selected a more aggressive clone of the primary tumor. The next step will be the comparison, from the molecular point of view, of the same established cell lines grown in 3D condition and we will evaluate other markers correlated with the tumor stroma interaction.

Conclusion

In conclusion, with this project we demonstrated that the brain matrix could play a pivotal role in the microenvironment of brain tumors. For this reason, it is strictly important to model *in vitro* the crosstalk between brain cancer cell and matrix proteins in a 3D condition, since it can reproduce a hypoxic core and it can better characterize the molecular mechanisms underline the aggressive and stemness tumor profile. Our model needs to be implemented with primary culture analysis, and different protein ratio. Moreover, it would need to be completed with two other proteins analyzed, fibronectin and laminin to increase its translational value. However, it is a first step in the development of a 3D model of brain tumors, which would enable the study and a more comprehensive delineation of the progression, and clinical evolution of gliomas.

Bibliography

1. *Brain Tumor: Statistics | Cancer.Net. https://www.cancer.net/cancer-types/brain-tumor/statistics.*

2. *di Nunno, V.* et al. *Tumor-Associated Microenvironment of Adult Gliomas: A Review.* Front Oncol ***12****, 3164 (2022).*

3. *Ostrom, Q. T.* et al. *Editor's choice: The epidemiology of glioma in adults: a "state of the science" review.* Neuro Oncol ***16****, 896 (2014).*

4. *Korbecki, J., Kojder, K., Grochans, S., Cybulska, A. M. & Simi, D. Epidemiology of Glioblastoma Multiforme – Literature Review. (2022).*

5. *Hsu, J. B. K., Chang, T. H., Lee, G. A., Lee, T. Y. & Chen, C. Y. Identification of potential biomarkers related to glioma survival by gene expression profile analysis.* BMC Med Genomics ***11****, (2019).*

6. *Byun, Y. H. & Park, C.-K. Classification and Diagnosis of Adult Glioma: A Scoping Review.* Brain & NeuroRehabilitation ***15****, (2022).*

7. *Weller, M.* et al. *EANO guidelines on the diagnosis and treatment of diffuse gliomas of adulthood.* Nat Rev Clin Oncol ***18****, 170–186 (2021).*

8. *Louis, D. N.* et al. *The 2021 WHO classification of tumors of the central nervous system: A summary.* Neuro Oncol ***23****, 1231–1251 (2021).*

9. *van den Bent, M. J. & Chang, S. M. Grade II and III Oligodendroglioma and Astrocytoma.* Neurol Clin ***36****, 467–484 (2018).*

10. *Lacerda, S., Neumaier, F., Zlatopolskiy, B. D. & Neumaier, B. Mutated Isocitrate Dehydrogenase (mIDH) as Target for PET Imaging in Gliomas.* Molecules 2023, Vol. 28, Page 2890 ***28****, 2890 (2023).*

11. *Capper, D.* et al. *DNA methylation-based classification of central nervous system tumours.* Nature 2018 555:7697 ***555****, 469–474 (2018).*

12. *Chai, R.* et al. *Molecular pathology and clinical implications of diffuse glioma.* Chin Med J (Engl) ***135****, 2914 (2022).*

13. *Koh, I. & Kim, P. In Vitro Reconstruction of Brain Tumor Microenvironment.* Biochip J ***13****, 1–7 (2019).*

14. *Faisal, S. M.* et al. *The complex interactions between the cellular and non-cellular components of the brain tumor microenvironmental landscape and their therapeutic implications.* Front Oncol ***12****, 5434 (2022).*

15. *Samanipour, R.* et al. *A review on 3D printing functional brain model.* Biomicrofluidics ***16****, (2022).*

16. *Chintala, S. K. & Rao, J. K. Invasion of human glioma: role of extracellular matrix proteins.* Front Biosci ***1****, (1996).*

17. *Lv, D.* et al. *A three-dimensional collagen scaffold cell culture system for screening anti-glioma therapeutics.* Oncotarget ***7****, 56904 (2016).*

18. *Bonneh-Barkay, D. & Wiley, C. A. Brain Extracellular Matrix in Neurodegeneration.* Brain Pathology ***19****, 573 (2009).*

19. *Wade, A.* et al. *Proteoglycans and their roles in brain cancer.* FEBS Journal ***280****, 2399–2417 (2013).*

20. *Huang, J.* et al. *Extracellular matrix and its therapeutic potential for cancer treatment.* Signal Transduction and Targeted Therapy 2021 6:1 ***6****, 1–24 (2021).*

21. *Martínez-Ramos, C. & Lebourg, M. Three-dimensional constructs using hyaluronan cell carrier as a tool for the study of cancer stem cells.* J Biomed Mater Res B Appl Biomater ***103****, 1249–1257 (2015).*

22. *Pibuel, M. A., Poodts, D., Díaz, M., Hajos, S. E. & Lompardía, S. L. The scrambled story between hyaluronan and glioblastoma.* Journal of Biological Chemistry ***296****, 100549 (2021).*

23. *Klank, R. L.* et al. *Biphasic Dependence of Glioma Survival and Cell Migration on CD44 Expression Level.* Cell Rep ***18***, *23–31 (2017).*

24. *Walker, C., Mojares, E. & Del Río Hernández, A. Role of Extracellular Matrix in Development and Cancer Progression.* International Journal of Molecular Sciences 2018, Vol. 19, Page 3028 ***19***, *3028 (2018).*

25. *Oldak, L.* et al. *Laminin-5, Fibronectin, and Type IV Collagen as Potential Biomarkers of Brain Glioma Malignancy.* Biomedicines 2022, Vol. 10, Page 2290 ***10***, *2290 (2022).*

26. *Chen, C. W.* et al. *The Fibronectin Expression Determines the Distinct Progressions of Malignant Gliomas via Transforming Growth Factor-Beta Pathway.* International Journal of Molecular Sciences 2021, Vol. 22, Page 3782 ***22***, *3782 (2021).*

27. *Orend, G. & Chiquet-Ehrismann, R. Tenascin-C induced signaling in cancer.* Cancer Lett ***244***, *143–163 (2006).*

28. *Yoshida, T., Akatsuka, T. & Imanaka-Yoshida, K. Tenascin-C and integrins in cancer.* https://doi.org/10.1080/19336918.2015.1008332 ***9***, *96–104 (2015).*

29. *Zhang, Q.* et al. *Tenascin C Promotes Glioma Cell Malignant Behavior and Inhibits Chemosensitivity to Paclitaxel via Activation of the PI3K/AKT Signaling Pathway.* Journal of Molecular Neuroscience ***71***, *1636–1647 (2021).*

30. *Domogatskaya, A., Rodin, S. & Tryggvason, K. Functional Diversity of Laminins.* https://doi.org/10.1146/annurev-cellbio-101011-155750 ***28***, *523–553 (2012).*

31. *Belousov, A.* et al. *The Extracellular Matrix and Biocompatible Materials in Glioblastoma Treatment.* Front Bioeng Biotechnol ***7***, *341 (2019).*

32. *Virga, J.* et al. *Extracellular matrix differences in glioblastoma patients with different prognoses.* Oncol Lett ***17***, *797 (2019).*

33. *Virga, J.* et al. *The Expressional Pattern of Invasion-Related Extracellular Matrix Molecules in CNS Tumors.* Cancer Invest ***36***, *492–503 (2018).*

34. *Virga, J.* et al. *Differences in extracellular matrix composition and its role in invasion in primary and secondary intracerebral malignancies.* Anticancer Res ***37***, *4119–4126 (2017).*

35. *Ruiz-Garcia, H.* et al. *Development of Experimental Three-Dimensional Tumor Models to Study Glioblastoma Cancer Stem Cells and Tumor Microenvironment.* Methods in Molecular Biology ***2572***, *117–127 (2023).*

36. *Ruiz-Garcia, H., Alvarado-Estrada, K., Schiapparelli, P., Quinones-Hinojosa, A. & Trifiletti, D. M. Engineering Three-Dimensional Tumor Models to Study Glioma Cancer Stem Cells and Tumor Microenvironment.* Front Cell Neurosci ***14***, *298 (2020).*

37. *Tang, M., Rich, J. N. & Chen, S. Biomaterials and 3D Bioprinting Strategies to Model Glioblastoma and Blood-Brain Barrier.* Adv Mater ***33***, *e2004776 (2021).*

38. *Jia, W.* et al. *Effects of three-dimensional collagen scaffolds on the expression profiles and biological functions of glioma cells.* Int J Oncol ***52***, *1787–1800 (2018).*

39. *Wang, X.* et al. *Reciprocal Signaling between Glioblastoma Stem Cells and Differentiated Tumor Cells Promotes Malignant Progression.* Cell Stem Cell ***22***, *514-528.e5 (2018).*

40. *Tang-Schomer, M. D.* et al. *3D patient-derived tumor models to recapitulate pediatric brain tumors In Vitro.* Transl Oncol ***20***, *(2022).*

41. *Tang-Schomer, M. D.* et al. *Bioengineered functional brain-like cortical tissue.* Proc Natl Acad Sci U S A ***111***, *13811–13816 (2014).*

42. *Friedrich, J., Seidel, C., Ebner, R. & Kunz-Schughart, L. A. Spheroid-based drug screen: considerations and practical approach.* Nature Protocols 2009 4:3 ***4***, *309–324 (2009).*

43. *Mirab, F., Kang, Y. J. & Majd, S. Preparation and characterization of size-controlled glioma spheroids using agarose hydrogel microwells.* PLoS One ***14***, *e0211078 (2019).*

44. *de Witt Hamer, P. C.* et al. *The genomic profile of human malignant glioma is altered early in primary cell culture and preserved in spheroids.* Oncogene 2008 27:14 ***27**, 2091–2096 (2007).*

45. *Hubert, C. G.* et al. *A three-dimensional organoid culture system derived from human glioblastomas recapitulates the hypoxic gradients and cancer stem cell heterogeneity of tumors found in vivo.* Cancer Res ***76**, 2465 (2016).*

46. *Mallick, K. K. & Cox, S. C. Biomaterial scaffolds for tissue engineering.* Frontiers in Bioscience - Elite ***5 E**, 341–360 (2013).*

47. *Xiao, W.* et al. *Bioengineered scaffolds for 3D culture demonstrate extracellular matrix-mediated mechanisms of chemotherapy resistance in glioblastoma.* Matrix Biology ***85–86**, 128–146 (2020).*

48. *Florczyk, S. J.* et al. *Porous chitosan-hyaluronic acid scaffolds as a mimic of glioblastoma microenvironment ECM.* Biomaterials ***34**, 10143–10150 (2013).*

49. *Chen, L.* et al. *The enhancement of cancer stem cell properties of MCF-7 cells in 3D collagen scaffolds for modeling of cancer and anti-cancer drugs.* Biomaterials ***33**, 1437–1444 (2012).*

50. *Wang, X.* et al. *Enrichment of glioma stem cell-like cells on 3D porous scaffolds composed of different extracellular matrix.* Biochem Biophys Res Commun ***498**, 1052–1057 (2018).*

51. *Mariappan, A., Goranci-Buzhala, G., Ricci-Vitiani, L., Pallini, R. & Gopalakrishnan, J. Trends and challenges in modeling glioma using 3D human brain organoids.* Cell Death & Differentiation 2020 28:1 ***28**, 15–23 (2020).*

52. *Sood, D.* et al. *3D extracellular matrix microenvironment in bioengineered tissue models of primary pediatric and adult brain tumors. doi:10.1038/s41467-019-12420-1.*

53. *Liverani, C.* et al. *A biomimetic 3D model of hypoxia-driven cancer progression.* Sci Rep ***9**, (2019).*

54. *Liverani, C.* et al. *Investigating the Mechanobiology of Cancer Cell–ECM Interaction Through Collagen-Based 3D Scaffolds.* Cell Mol Bioeng ***10**, 223 (2017).*